University of Thessaly
School of Health Sciences
Department of Biochemistry and Biotechnology

# MicroRNAs deregulation in cancer

## MicroRNA mediated regulation of PARN: a cancer related ribonuclease

Papikinos Konstantinos

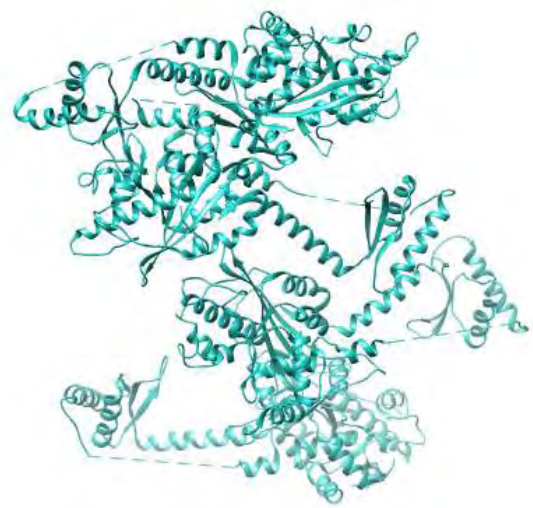

# Απορρύθμιση των microRNA στον καρκίνο

## Ηρύθμιση της PARN από τα microRNA: μία σχετιζόμενη με τον καρκίνο ριβονουκλεάση

*Trento, Italy 2014*

*ACKNOWLEDGEMENT*

*First and foremost, I have to thank my research supervisor and the committee, Ms. Michela Alessandra Denti, Mr. Nikolaos Balatsos and Mr. Demetrios Leonidas. Without their assistance and dedicated involvement in every step throughout the process, this paper would have never been accomplished. I would like to thank you very much for your support and understanding over these past four years.*

*Getting through my dissertation required more than academic support, and I have many, many people to thank for listening to and, at times, having to tolerate me over the past four years. I cannot begin to express my gratitude and appreciation for their friendship. I want to thank every one of my professors for they have been unwavering in their personal and professional support during the time I spent at the University. I must also thank my colleague at the CiBio lab of RNA Biology & Biotechnology, Dr. Valerio Del Vescovo, for giving me opportunity to develop as a scientist and to gain the necessary confidence for my work.*

*Most importantly, none of this could have happened without my family. My father, my mother and my sister who offered their encouragement through phone calls and long talks – despite my own limited devotion to correspondence. To my parents and my sister– it would be an understatement to say that, as a family, we have experienced some ups and downs in the past four years. Every time I was ready to quit, you did not let me and I am forever grateful. This dissertation stands as a testament to your unconditional love and encouragement even in the darkest times.*

| ***Supervisor:*** | ***Co-supervisor:*** | ***Member:*** |
|---|---|---|
| ***Michela Alessandra Denti*** | ***Nikolaos Balatsos*** | ***Demetrios Leonidas*** |
| Assistant professor of Molecular Biology | Assistant Professor of Biochemistry | Associate Professor of Biochemistry |

# 1. Περίληψη

Τα microRNA είναι μικρά μη-κωδικά ολιγονουκλεοτίδια μήκους περίπου 20-25 ζευγών βάσεων. Ρυθμίζουν την γονιδιακή έκφραση στο μετά-μεταγραφικό επίπεδο μέσω της πρόσδεσης τους στα μετάγραφα στο κυτταρόπλασμα. Η πρόσδεση εξαρτάται από την συμπληρωματικότητα των δύο νουκλεϊκών οξέων. Η PARN (PARN, EC 3.1.13.4) είναι μία υδρολάση που δρα σε εστερικούς δεσμούς και παράγει 5'-φωσφομονοεστέρες. Ειδικότερα, η PARN είναι μια αποαδενυλάση που αποικοδομεί ειδικά τις πολυ(Α) ουρές των mRNAs με κατεύθυνση 5΄- 3΄. Η PARN είναι πολύ σημαντική για την αποικοδόμηση των mRNAs στα ευκαρυωτικά κύτταρα και για την σωστή ανακύκλωση των mRNAs. Η PARN μπορεί πιθανά να δρα και ως ογκοκατασταλτικός παράγοντας προκαλώντας την αποικοδόμηση των mRNAs της IL-8 και του VEGF. Τα miRNA αποτελούν επίσης παράγοντες-κλειδιά στην ρύθμιση της ανακύκλωσης των mRNA. Με την αλληλεπίδραση τους μέσω της συμπληρωματικότητας αφενός παρεμποδίζουν την μετάφραση αφετέρου προκαλούν την αποικοδόμηση του mRNA στόχου προσελκύοντας ριβονουκλεάσες, όπως η PARN. Στην παρούσα μελέτη εξετάζουμε πως η PARN ρυθμίζεται από τα miRNAs. Εξετάσαμε το ρόλο των miR-29a-3p και miR-1207-5p στην έκφραση της PARN. Παρατηρήσαμε πως τα εν λόγω miRNAs έχουν την ικανότητα να προσδένονται στην 3' αμετάφραστη περιοχή της PARN και να προκαλούν μείωση της εκφρασης της. Πιστοποιήσαμε τις αλληλεπιδράσεις μέσω της παραγωγής μεταλλαγμάτων της 3' αμετάφραστης περιοχής της PARN για τις θέσεις πρόσδεσης των miRNA.

# 1. Abstract

MicroRNAs (miRNA) are small non-coding oligonucleotides of about 20-25 base pairs in length. They have the ability to regulate gene expression at the post-transcriptional level by binding onto transcripts in the cytoplasm in sequence specific manner. Poly(A)-specific ribonuclease (PARN, EC 3.1.13.4) is a hydrolase that acts on ester bonds and produces 5'-phosphomonoesters. Specifically, PARN is a deadenylase that degrades the poly(A)-tails of the m-RNAs with a 5'-3' direction. PARN is very important for the degradation of mRNAs in the eukaryotic cells and for the correct turnover of the mRNAs. PARN can potentially act as a tumor suppressor causing degradation of IL-8 and VEGF mRNAs. miRNAs are also key players in the regulation of miRNA turnover. With a sequence specific manner they can prevent translation or even degrade their target mRNA. In this later step of degradation miRNAs can recruit ribonucleases, like PARN, to help them degrade the transcripts. In this study we examine how PARN is being regulated by miRNAs. We examined how the expression of PARN is regulated under the influence of miR-29a-3p and miR-1207-5p. We were able to notice that these two miRNAs have the ability to bind to the 3' UTR of PARN and cause the decrease in the expression levels. We verified also these interactions by creating mutants of the original 3' UTR for the sites for the miRNAs.

## Table of Contents

# 2. Introduction

## 2.1. *microRNAs*

MicroRNAs (miRNA) are small non-coding oligonucleotides of about 20-25 base pairs in length. They have the ability to regulate gene expression at the post-transcriptional level by binding onto transcripts in the cytoplasm in sequence specific manner. The actual repression occurs wither by degradation of the target transcript or through inhibition of the translational process. They were discovered two decades ago by Ambros et al[1] and changed the focus of the scientific community from the classical central dogma of biochemistry[2]. For the first time the focus was turned over to non-coding genes and in the next twenty years our knowledge around miRNAs and the biological role has expanded and keeps giving us new insights.

The first miRNA was found in *C. elegans.* Ambros and colleagues discovered *lin-4* a gene that was found to encode for the production of two small RNAs which also are complementary to the 3' untranslated region of *lin-14* mRNA[1]. One of these transcripts was 61 base pairs long and found to create a stem loop and the other was about 21 nucleotides long. It was also found that the levels of the LIN-14 protein were reduced when these RNAs were present and allowed the larva to proceed from developmental stage 1 to 2. These discoveries suggested that there was an RNA-RNA interaction that caused this specific post-transcriptional suppression of *lin-14*[1].

Seven years later in 2000 *let-7* become the second miRNA to be discovered by Reinhart et al again in *C. elegans*[2,3]. It was characterized as a 21 nucleotide long RNA that controlled the L4 to adult transition of the larva. The remarkable in this case is the discovery that *let-7* is conserved across species, even in humans, and triggered the quest to find other molecules like that and also upgraded the importance that miRNAs may have and their role[2].

Nowadays it is known that miRNAs represent almost 1% of the genome of many species and estimations show that 30% of our genes are regulated by at least one miRNA[4,5]. Current release 20 of miRBase[6], a database hosted by the University of Manchester and supported by the Welcome Trust Sanger Institute, hosts 24,521 entries of predicted hairpin structures of miRNAs and provides information such as the position and the sequence.

## 2.2. *microRNAs biogenesis and role in cancer*

MiRNAs are dispersed along our genome and as already stated before they represent about 1% of our genome. The genes that produce miRNAs can be found as single genes or as clusters that can either be transcribed independently from one another or as polycistronic transcripts. Furthermore the genes can also be part of the introns of a gene that transcribes for the mRNA.

MicroRNA biogenesis is a process that involves many stages of maturation. The birth of miRNAs takes place in the nucleus where miRNA genes transcribe and produce one long transcript. This is called pri-miRNA and is the primary precursor of the final about 21 base pair long miRNA[2]. Pri-miRNA is both 3' adenylated and bears a 7-methylguanosine cap[7]. The transcription is carried out by RNA-polymerase II and rarely by RNA-polymerase III[7–9]. The transcript that is created can contain only one miRNA but can in some cases be polycistronic and contain the sequences of more than one miRNAs. The transcription is also under the control of transcription factors of the cell and of the methylation of the promoters[10–12].

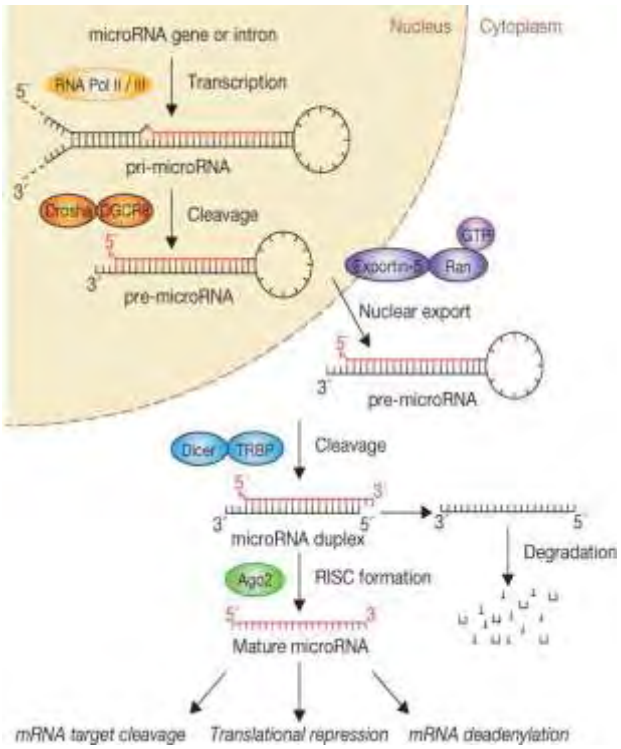


**Figure 1 miRNA biogenesis[66].**

Then it is time for Drosha to process the pri-miRNA and to allow it to proceed to the next step. Drosha is a class 2 RNase III enzyme and is part of the *Microprocessor complex* along with the dsRNA binding protein DGCR8[13]. After this the transcript is now the precursor pre-miRNA and has a hairpin structure of 60-110 nucleotides in length[2,13]. It also now has a 2 nucleotide overhang in the 3' due to its cleavage from an RNase III[13]. The last step for the pre-miRNA in the nucleus is their transfer to the cytoplasm. in this step the processed transcript uses the RanGTP/exportin 5-dependent mechanism[14–16]. It has been stated in the literature that for the export from the nucleus the ends created in the previous step from Drosha may facilitate a better interaction between the miRNA and the exportin complex[15]. However it is worth to note that there are also some miRNAs that contain special sequences that imply their sub cellular localization as shown in 2007 by

Hwang et al[17]. In some cases some miRNAs contained signals that led them back to the nucleus.

In the cytoplasm the transcript has to undergo some more modifications in order to become mature. The first step is the cleavage from another RNase III. This time it is Dicer-1, together with TRBP/PACT proteins, that will cleave the pre-miRNA hairpin in an imperfect RNA duplex of about 20-21 nucleotides long[18–20]. Finally the duplex will be unwound by a helicase into a one stranded mature miRNA that is ready to proceed to the next stage and be used by the cell mechanism in order to induce its effect[21]. We have to note that from the helicase reaction two possible miRNAs normally are created but eventually only one is being chosen and loaded onto the RNA-induced silencing complex. Usually the strand with the most unstable base pair on its 5' end is the one loaded as it is stated in the literature[22,23].

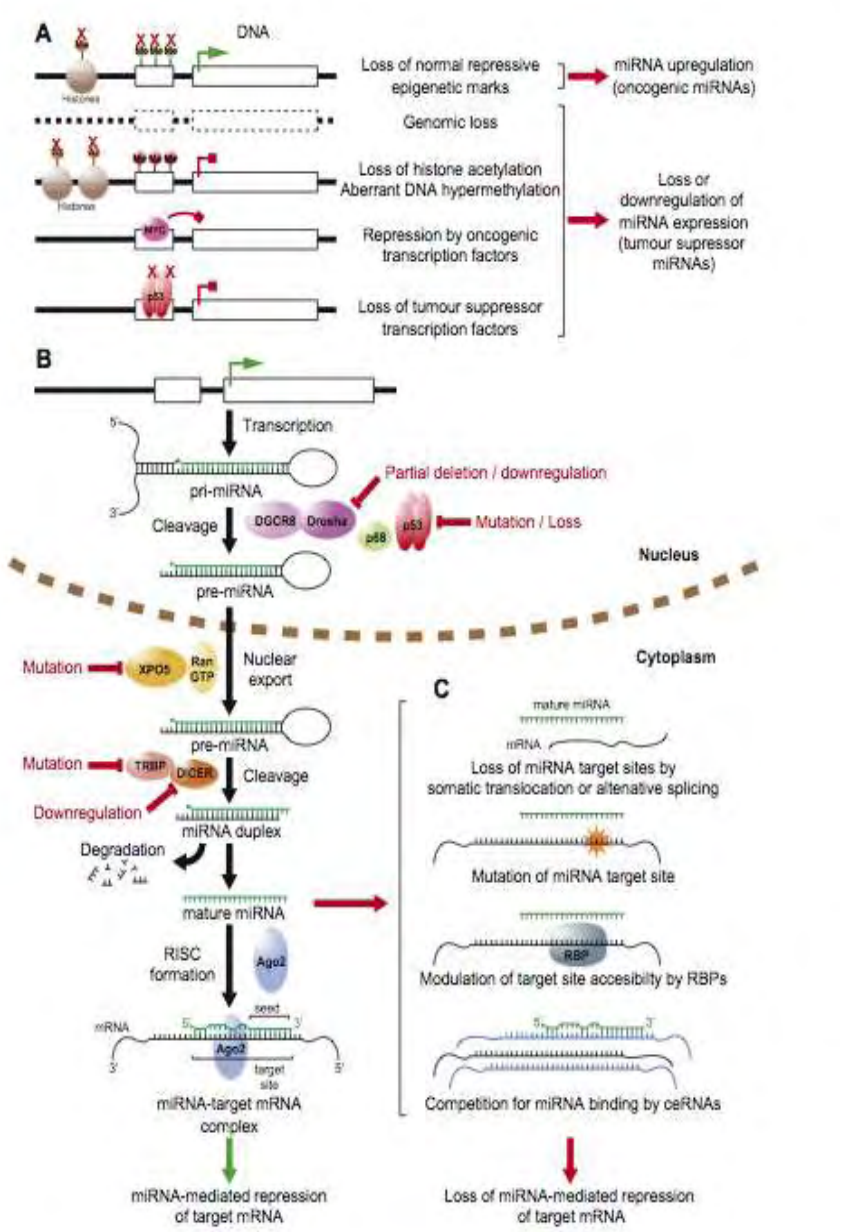


**Figure 2 Figure of the miRNA biogenesis and action pathway enriched with all the possible changes that could lead to miRNA deregulation in the organism in the case of cancer. (A) shows deregulation in the gene level. (B) deregulation in the biogenesis process or during the canonical pathway. (C) mechanisms with witch cancer can allow the cell to skip the regulation of miRNAs[26].**

Deregulation can be noticed in many different levels of the biogenesis pathway of miRNAs. Just like protein-coding genes in cancer a miR-gene can be deregulated in many different ways. In this thesis we will only provide a quick view to all these mechanisms.

First in the list are mutations of the miRNA. It is easily understandable that a mutation of the seed site of the mature miRNA could cause the complementarity loss and thus inhibit the control of a oncogene.

Cancer cells undergo a series of epigenetic changes like hyper-methylation etc[24]. Lots of miR-genes have been found to be associated with CpG islands and so epigenetics could alter the expression of miR-genes in cancer[25]. miRNA expression can be affected by the presence or absence of transcription factors. Oncogenic factors like Myc have been found to cause the suppression of tumor-suppressing miRNAs. Respectively transcription factors that are tumor-suppressors usually induce the biogenesis of miRNAs that enable tumor-suppression. In cancer many of these factors are no longer expressed and so the expression of these miRNAs is also deregulated.

Another way to deregulate miRNAs is by mutations in the biogenesis pathway. As we discussed before the biogenesis of miRNAs is a complex pathway that includes many proteins and many steps to complete. A mutation that causes loss of function in such a protein can lead to a problem in the biogenesis of miRNAs and thus can result in no miRNA production[26–28].

The reason for the loss of regulation can also be the target: a mutation could create an isoform of the mRNA that for some reason (alternative splicing, point mutation) is no longer susceptible to the control of the miRNA[26].

### 2.3. *microRNAs as therapeutic agents*

It is evident that miRNAs have the ability to regulate a large number of genes. It is also valid to think that many diseases are based on the deregulation of certain genes that cause the phenotype. So immediately we raise a point where miRNAs can be possibly manipulated in such way that we could use them to restore the normal condition. This thought exists in the literature already. There some trials in cell lines, rodents and non-human primates that suggest that it may be possible to produce a certain phenotype and eventually lead us to new ways of fighting diseases[29–32]. The uses seem to have a broad range from obesity to cancer and even to viral infections[33].

Another approach is to use miRNAs as biomarkers[2]. That can either help us distinguish people in healthy and disease groups or can be used as markers of the progression of a disease. Special interest exists in miRNAs in the serum since it is a non-invasive sample

that is easily received from patients[2]. Especially about cancer certain deregulations of miRNAs in the plasma have been reported in the literature[34–37].

## 2.4. *PARN and its role in cancer*

Poly(A)-specific ribonuclease (PARN, EC 3.1.13.4) is a hydrolase that acts on ester bonds and produces 5'-phosphomonoesters. *PARN* gene is located on chromosome 16p13.The human protein is a homodimer and has high specificity for poly(A) tails. This specificity comes from the residues of the active site and the nucleotides around the actual acting site regulate the efficiency of the enzyme. It has 639 amino acids and weighs 74 kDa[38]. PARN acts as a homodimer and its active site consists of four acidic amino acids Asp28, Glu30, Asp292, and Asp382[39–41]. The amino acids that form the active site are also characteristic of the family of the enzyme. PARN is part of the RNase D family which is part of the DEDD superfamily[39–41]. The formation of the homodimer is essential for the catalytic activity of the enzyme[42,43]. It has 3 domains: the catalytic nuclease, the R3H domain and the RNA binding domain[42–44].

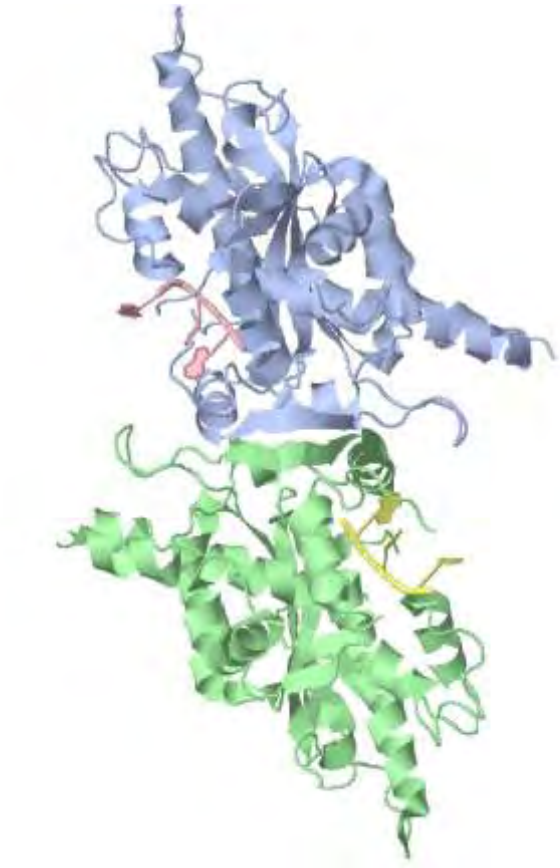

**Figure 3 The 3D structure of the nuclease domain of PARN from Protein Data Bank Database**

PARN is very important for the degradation of mRNAs in the eukaryotic cells and for the correct turnover of the mRNAs. The step of deadenylation is crucial for the 3'➔5' decay. Besides this PARN plays a role in **N**on-sense **M**ediated **D**ecay (NMD)[45] of transcripts that contain a premature stop codon, in the maturation of oocytes[46–48], in the embryonic development[49], in the degradation of unstable mRNAs rich in AU[50] and in DNA repair[51,52]. It is an enzyme highly conserved among many eukaryotes. Another unique feature of PARN is the fact that is the only deadenylase that interacts not only with the

poly(A) tail but also with the m$^7$G-cap. PARN also plays a role in the biogenesis of some miRNAs like miR-451[53].

The information on the biological role and the regulation of PARN in cancer is very limited. PARN can potentially act as a tumor suppressor causing degradation of IL-8 and VEGF mRNAs. Importantly, RBPs such as KSRP, tristetraprolin (TTP) and CUG-BP may recruit PARN to destabilize various mRNAs, including *c-jun*, uPA, *c-fos* and TNF mRNAs, the elevations of which are implicated in cancers[54]. Recent work has shown that the expression of several deadenylases in altered in acute leukemias, while PARN may represent a promising biomarker[55]. Further, preliminary results from the lab of Mr. Nikolaos Balatos' lab from pathological samples suggest that PARN and several deadenylases are differentially expressed in lung cancer subtypes, including squamous cell carcinoma and small cell lung cancer.

## 2.5. *mRNA stability in cancer and miRNA mediated deadenylation*

One of the hallmarks of cancer is the mRNA instability. In many cancers abnormalities in the regulation of gene expression and mRNA stability are present[54]. Normally the degradation of the transcripts in the cells are under strict control through cellular signals[56–58].

Studies in the last decade have shown that this deregulation is not only part of amplifications, deletions or problems in critical cellular processes but can be also due to components of the post-transcriptional mechanism[54]. *Cis*-acting and

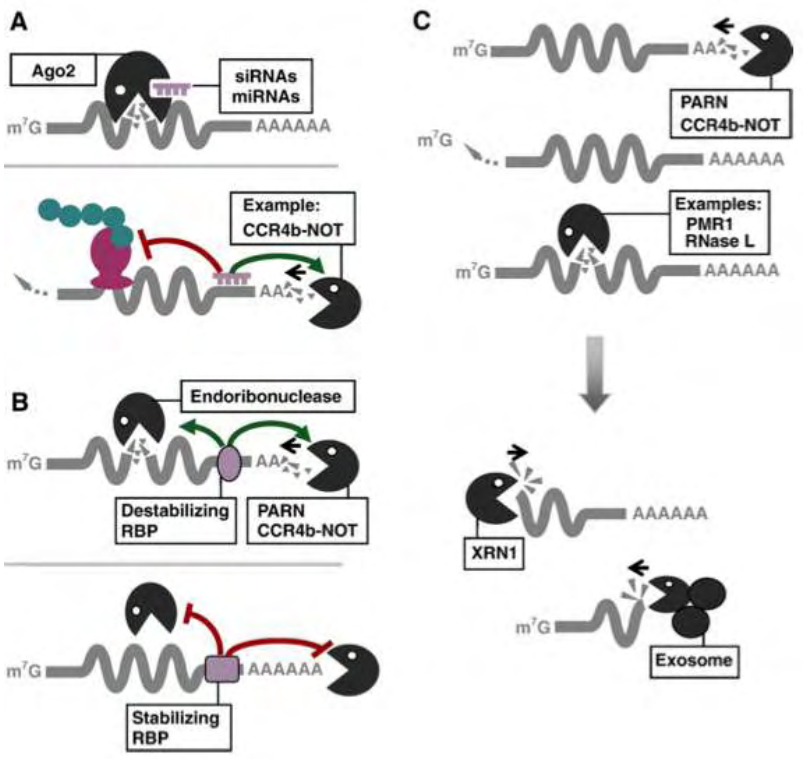


**Figure 4 Modes of action for trans-acting factors. (A) Non-coding RNAs can regulate mRNA translation and degradation. Top: Argonaute 2 (Ago2) is induced to cleave mRNAs with externally introduced short interfering RNAs (siRNAs). However, a near to perfect complementary hybridization of miRNAs to mRNAs can also induce Ago2, complexed with other gene silencing machineries, to cleave the target mRNA. Bottom: miRNAs, a subclass of non-coding RNA, can inhibit the translational process while recruiting the RNA decaying machineries such as deadenylases and decapping enzymes. (B) RNA-binding protein (RBP) controls the stability of mRNAs. (C) Ribonucleases (RNases) can act alone or in concert with other decaying factors to destine mRNAs for degradation. Deadenylases such as Poly A Ribonuclease (PARN) and CCR4b from CCR4b–NOT complex remove the Poly A tail of the target mRNA, while decapping enzymes remove the 5′-m7G mRNA cap. Endoribonucleases can cleave mRNA in the middle of mRNA sequence. The combinations of these three processes make mRNA available for exoribonucleases to further degrade and clear the transcript in 5′–3′ (XRN1) or in 3′–5′ direction (Exosome complex)[54].**

*trans*-acting elements may play a role especially in the degradation of the mRNA. In this context non-coding RNAs like miRNAs and ribonucleases like PARN may be implicated in the process of tumorigenesis.

For miRNAs the main mode of action is their interaction with the 3' UTR of the mRNA. Through the complementarity between the miRNA and the mRNA proteins of the Argonaute family (Ago) are recruited forming a complex with the miRNA inhibiting translation[54]. In some cases of almost complete complementarity the result can be the endonucleolytic cleavage of the transcript. Of all the members of the Argonaute family only Ago2 has been found to have the ability to induce this cleavage through its RNase H domain[59,60]. miRNAs can also induce degradation of the mRNA through a deadenylation-dependent manner or independent exonucleolytic pathway, or by unidentified decay factors as show in figure 5 A through the recruitment of deadenylases like CCR4b[54]. Especially about deadenylation induced by miRNAs, they recruit the miRNA-induced silencing complex (miRISC), which includes Argonaute and GW182 as core proteins[61]. GW182 proteins effect translational repression and deadenylation of target mRNAs. GW182 independently tethers two deadenylase machineries (CCR4–NOT and PAN2 and PAN3) by means of independent motifs and has a newly identified role as a deadenylase coactivator in the processive deadenylation of mRNA targets[61]. Firstly, GW182 serves as a binding platform that recruits two deadenylase complexes to target RNAs. Secondly, GW182 acts as a deadenylation coactivator by assisting the CCR4–NOT complex to shorten the poly(A) tail[61].

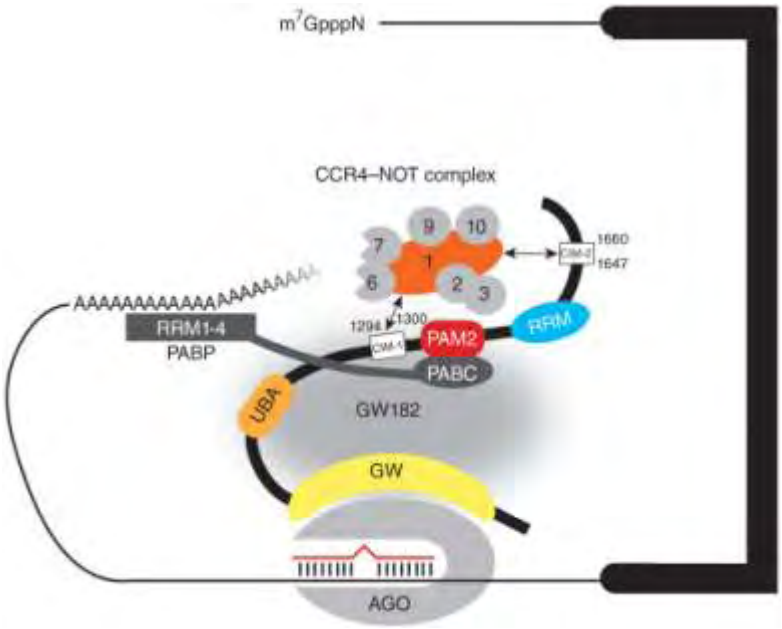


**Figure 5 GW182 binds Argonaute (AGO) through its N-terminal GW-rich domain to form the miRISC. GW182 recruits the poly(A) tail into the vicinity of the miRISC by interacting with PABP through the PAM2/PABC contact. Two CCR4–NOT interaction motifs (CIMs) in the GW182 recruit the CCR4–NOT complex to facilitate deadenylation of miRNA-targeted mRNAs. CIM-1 and CIM-2 are labeled with their coordinates in the human GW182 paralog TNRC6C. The CNOT1 subunit interaction with GW182 is depicted with two-sided arrows. The PAN2–PAN3 interaction with PABP has been purposely excluded to simplify the figure.**[61]

Moreover RNA binding proteins can affect mRNA stability. These proteins have the ability to bind on the transcripts either on the 3'UTR or the coding region and regulate the

degradation rate of a transcript[62–64]. Depending on the protein, as shown in figure 5 B, the effect can be destabilization, through the recruitment of ribonucleases, or stabilization of the transcript through inhibition of the action of these enzymes.

mRNA stability and degradation can be regulated by the action of exoribonucleases[65]. They can induce the deadenylation of the transcript and the degradation from the 3' to the 5' end: PARN is protein that can act in this way. Moreover the removal of the cap can allow exoribonucleases to digest the mRNA from 5' to 3' end. Finally endoribonucleases internally digest the transcripts. The resulting fragments are further degraded by exoribonucleases without requiring the deadenylation or the decapping step[54].

In cancer these mechanisms may be deregulated resulting in an abnormal regulation of the mRNA and altered turnover time. The result is a change in the levels of different transcripts in the cells. Some of these transcripts may act as oncogenes or tumor suppressors therefore the loss of the cells' equilibrium can lead to tumorigenesis and cancer progression.

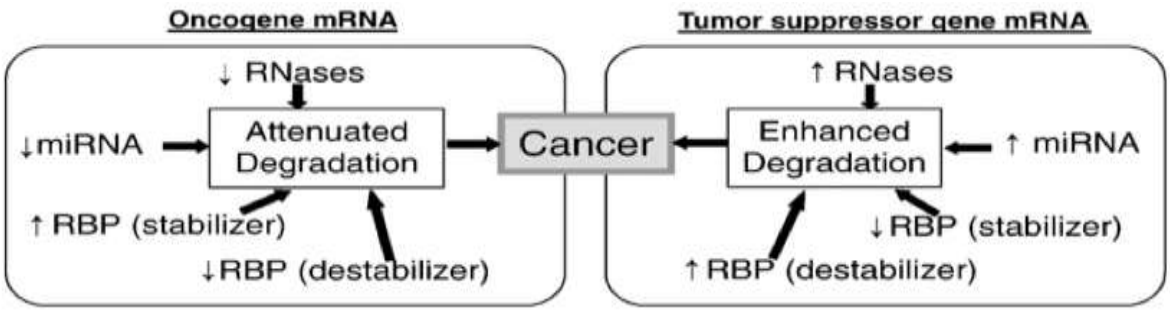


**Figure 6 Depending on the nature of the mRNA (oncogene or tumor supressor) the loss of mRNA regulation can lead to a prolonged exposure of the cell to factors that lead to the cration of a cancer cell[54].**

# 3. Aim of this study

The aim of this study is to investigate the possible regulations of PARN by miR-29a-3p and miR-1207-5p. As mentioned before both miRNAs and PARN are considerable elements that allow the cell to control the expression of different transcripts at any time. These regulations are very important, especially for diseases like cancer that have their bases in deregulation of the cell cycle. Both of these miRNAs have been found to be deregulated when PARN is silenced. They also seem to have the ability to silence PARN proposing that a certain feedback loop may be present. We tried to investigate if there is really such an interaction between the enzyme's mRNA and the miRNAs. The study was part of my ERASMUS scholarship and was conducted at the Laboratory of RNA Biology and Biotechnology of the University of Trento, Italy.

# 4. Materials and methods

## 4.1. *Bioinformatics analysis*

From miRBase and Genome Browser we downloaded the sequence of our miRNAs and PARN's 3' UTR respectively. That way we were able to work in silico and predict target sites.

Using the PITA algorithm, software provided by Segal Lab of Computational Biology, on the 3' UTR of PARN we were able to identify 4 positions for our miRNAs of interest. Subsequently we entered the FASTA format of our 3' UTR and our miRNAs in the RNAHybrid tool and tried to identify the exact 7-mer or 8-mer of the binding region. We managed to locate seeds on all of the PITA predicted sites. Thanks to these information we could now divide the 3' UTR region into fragments, which were transfected into HeLa cells, containing our target sequences.

## 4.2. *Plasmids*

### 4.2.1. *pmirGLO* Dual-Luciferase miRNA Target Expression Vector *(Promega)*

pmirGLO is a specially designed vector by Promega that allows us to detect and measure the activity of the miRNAs by cloning our target 3´ of the firefly Luciferase gene (*luc2*). *Firefly* Luciferase is the primer reporter gene that will actually indicate if there is a reduction of signal. This vector also expresses the *Renilla* Luciferase (*hRluc-neo*), which is used to normalize the results. In Figure 6 you can see the map of the vector. The PGK promoter of the Firefly Luciferase offers the ability to have a more sensitive analysis than by the use of a strong promoter.

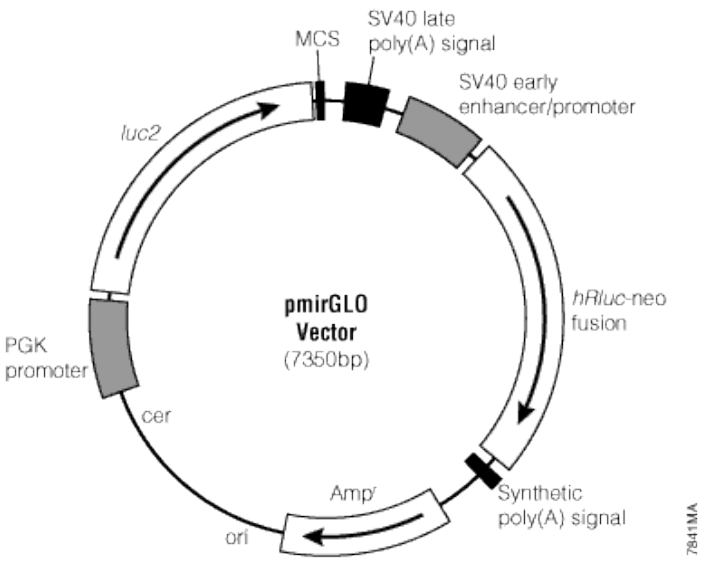


**Figure 7** ***pmirGLO*** **vector**

### 4.2.2. *psiUX Vector*

This vector was available in the RNA Biology and Biotechnology. It contains the Amp gene for selection and the precursor region of the miRNAs of interest. The pri-miRNA is cloned between the promoter and the terminator of the human U1 small RNA, which is highly transcribed. The use of this vector allowed us to achieve a physiological production of the mature miRNAs inside our cells.

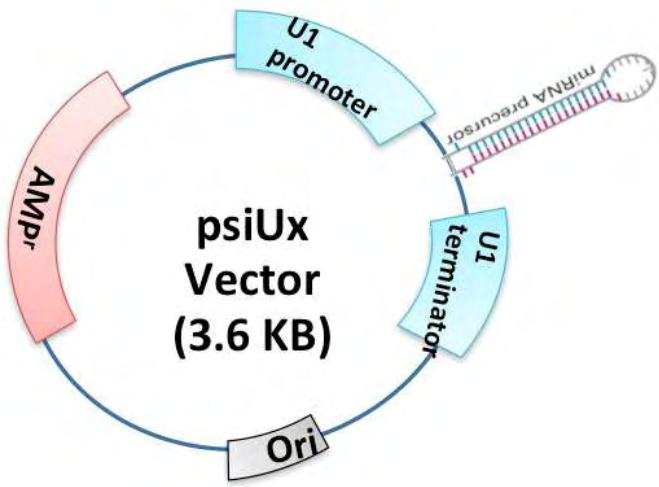


Figure 8 *psiUX* vector[67]

### 4.3. *E.coli transformation*

For the transformation of *E. coli* DH5a competent and XL10 ultra competent cells we thaw them in ice for 10 minutes. During this time we add our DNA (10µl for a ligation reaction) to 100µl of KCM buffer (100mM KCl, 30mM $CaCl_2$, 50mM $MgCl_2$) and keep in ice for 5 minutes. We then add 100µl of competent cells to the KCM-DNA mixture and gently mix. We incubate in ice for 20 minutes. Afterwards we heat shock the cells by exposing them to a temperature of 42°C for 1 minute and subsequently put them in ice for 1 minute. We add 800µl of Luria Broth and incubate at 37°C for 40 minutes in a shaking incubator with a speed of 140 rpm. After the incubation we spin our cells at 4000 rpm for 4 minutes to pellet them and remove 800µl of the mixture from the tube. We resuspend the cells in the remaining 200µl and plate 50-100µl of them on an appropriate plate. The plates are prepared using LB agar (Sigma) and ampicillin (50µg/ml). Plates are incubated overnight at 37°C and the next day a solid colony is picked up and inoculated in Luria Broth.

### 4.4. *Plasmid DNA extraction*

For the plasmid DNA extraction we used QIAGEN Plasmid Maxi Kit and QIAprep Spin Miniprep Kit. With the Maxi Kit we were able to extract plasmid DNA in high concentrations

from bacterial cultures of about 200 ml. The basis of the extraction is the anion-exchange tips for purification of transfection-grade plasmid DNA from the lysate of the bacterial cells. For the Maxi Kit we pellet the cells at 6000 x g for 15 minutes at 4°C and treat them with the 10ml of buffer P1 that is given with the kit, this allows us to resuspend the cells in an appropriate environment for the next steps. Then we add 10ml of the second buffer P2, which will induce the lysis of the bacterial cells, and we incubate for 5 minutes at room temperature. The addition of 10ml of P3 buffer results in the interruption of the lysis. After the neutralization we see the formation of debris from the cells like genomic DNA, proteins etc. We centrifuge for 5 minutes at 8000xg so that the debris precipitate and we get a clear lysate. We apply the lysate on the special syringe like column that is used to filter the lysate. We then add 2,5ml of the endotoxin removal buffer that is provided and incubate for 30 min on ice. We then equilibrate the anion exchange column using 10ml of a low salt buffer that is provided (Buffer QBT). We apply the lysate and allow the gravital forces to empty the column. We wash using 30ml of medium salt buffer (Buffer QC) twice and finally we elute the plasmid in 15ml of high salt buffer (Buffer QN). Subsequently we precipitate DNA by adding 10.5 ml room temperature eluted DNA. Mix and centrifuge immediately at ≥15,000 x g for 30 min at 4°C. This step is done in order to clean our DNA from the salt that is in the elution buffer. In the next step we wash the pelleted DNA with 70% ethanol, which removes precipitated salt and replaces isopropanol with the more volatile ethanol, making the DNA easier to redissolve. Finally we decant the supernatant and redissolve the DNA in 300μl of RNase DNase free water.

For the Spin Miniprep kit the procedure is simpler and instead of gravital forces it uses a tabletop microcentifuge. We pellet the cells at 8000 rpm for 4 min and then resuspend them in 250μl buffer P1. Then we add 250μl of buffer P2 to induce the lysis of the cells. To neutralize the reaction and stop the lysis we add the provided buffer N3. To clear the lysate from the debris we centrifuge for 10 minutes at 12000 rpm. Subsequently we apply the supernatant to the columns that contain a specialized silica membrane on which our DNA is binding. We centrifuge at 12000 rpm for 1 minute and discard the flow-through. We wash two times with 0,5ml and 0,75ml of the provided buffers PB and PE respectively. After the addition of each of the buffer we centrifuge for 1 minute at 12000 rpm and discard the flow through. After the PE buffer we centrifuge once again to clean the column from

any residues. Finally we add 50µl of water in the center of the column and place it in a 1,5 ml eppendorf. Centrifuge for one more minute to obtain our DNA.

**Table 1 Composition of buffers for plasmid extraction**

| Name of buffer | Composition |
|---|---|
| **P1** | 50 mM Tris-HCl pH 8.0, 10 mM EDTA, 100 µg/ml RNaseA |
| **P2** | 200 mM NaOH, 1% SDS |
| **P3** | 3.0 M potassium acetate pH 5.5 |
| **Buffer QBT** | 750 mM NaCl, 50 mM MOPS pH 7.0 ,15% isopropanol, 0.15% triton X-100 |
| **Buffer QC** | 1.0M NaCl, 50 mM MOPS pH 7.0, 15% isopropanol |
| **Buffer QN** | 1.6M NaCl, 50 mM MOPS pH 7.0, 15% isopropanol |
| **Buffer N3** | 4.2 M Gu-HCl, 0.9 M potassium acetate, pH 4.8 |
| **Buffer PB** | 5 M Gu-HCl, 30% isopropanol |
| **Buffer PE** | 10 mM Tris-HCl pH 7.5, 80% ethanol |

### 4.5. *Cloning*

Thanks to the bioinformatic analysis we had the ability to proceed with the cloning of the 3' UTR of PARN. We cloned the total 3' UTR and some fragments that we chose with our bioinformatic tools. First we had to design the primers for our region of interest. These primers are shown below along with a scheme of the 3' UTR of PARN and the relative location of our chosen fragments on it. Before amplifying anything we had to check the best annealing temperature for our primers. So we performed a PCR reaction using a

**Table 2 PCR primers for the amplification of the 3' UTR of PARN and fragments. Green indicates the restriction site for SacI-HF® and yellow for XhoI. Direction 5'➔3'**

| | |
|---|---|
| PARN29a FOR | **ACTGGAGCTCCCAAGACCTGAGGGCAGCAA** |
| PARN29a REV | **ACTGCTCGAGCAGGAGACAACTTGGTTTCC** |
| PARN1207 5p FOR | **ACTGGAGCTCCTGCTGTGATCATGAATTTG** |
| PARN1207 5p REV | **ACTGCTCGAGAAGGACAAGCTTGAGAGCGT** |
| PARN1207 5p-29a FOR | **ACTGGAGCTCCATGGGGGATGTACGAGTAA** |
| PARN1207 5p-29a REV | **ACTGCTCGAGTGCTGTGATCTGTTTCAACG** |
| PARN tot REV | **ACTGCTCGAGGTCCTATGAAAATGTTTTTA** |

temperature


**Figure 9 The relative positions of the fragments we created on the 3' UTR of PARN. In the grey rectangles you see the relative positions of the miRNA sites on the 3' UTR**

gradient (48,2°C-66°C) and set up multiple reactions in order to run them on an agarose gel and check the results. For this reaction the protocol was this:

**Table 3 PCR mix for the temperature gradient reaction volumes and protocol**

| Reagents | 1x | Run |
|---|---|---|
| **dNTP's** | 0,5 μl | 5:00 minutes 95°C |
| **Reaction Buffer 10x** | 3 μl | **0:30 seconds 95°C** |
| **RBC polymerase** | 0,3 μl | **0:40 seconds 66°C-44°C** |
| **Genomic DNA** | 1,5 μl | **1:00 minute 72°C** |
| **Primer FOR** | 1 μl | **Repeat x34** |
| **Primer REV** | 1 μl | 5:00 minutes 72°C |
| **Water** | 22,7 μl | 12°C Infinite |
| **Total** | 30 μl | |

The 30 μl reaction is separated in 10 μl smaller reactions and run in three different temperatures 48,2°C, 57,3°C and 64,2°C. This same reaction mix was used for the amplification of the 3' UTR in the ideal temperature for the primers. All the PCR products were checked by electrophoresis on an 1,5% agarose gel.

After the amplification we use a QIAGEN commercial kit for the purification of the PCR product. DNA adsorbs to the silica membrane in the presence of high concentrations of salt, while contaminants pass through the column. Impurities are efficiently washed away,

and pure DNA is eluted with water. Then the purified DNA from the PCR and our vector (pGLO) is restricted by the two enzymes of choice SacI-HF® and XhoI. For the restriction reaction we used:

**Table 4 Restriction mix for 3' UTR and vector**

| Reagents | PCR products | Vector | Protocol |
|---|---|---|---|
| **Reaction Buffer 10x** | 5,6 μl | 5 μl | 37°C for 3 hours |
| **XhoI** | 1 μl | 1 μl | |
| **SacI-HF®** | 1 μl | 1 μl | |
| **DNA** | The whole purified PCR product | 10 μl of a 1478 ng/μl | |
| **Water** | - | 33 μl | |

Then we purify again using the same kit to clean our DNA from any chemicals or enzymes that could possibly inhibit our ligation reaction. For the ligation we used the following protocol:

**Table 5 Ligation mix and protocol**

| Reagents | 1x | Protocol |
|---|---|---|
| **Reaction Buffer 10x** | 2 μl | Overnight incubation at room temperature and protected from light |
| **T4 DNA ligase** | 1 μl | |
| **3' UTR of PARN** | 35 ng | |
| **Vector** | 1 μl of a special dilution 100 ng/μl | |
| **Water** | Until total volume 20 μl | |

After the incubation we used 10 μl of the reaction to transform DH5α cells as discussed above.

### 4.6. *Site directed mutagenesis*

For the site-directed mutagenesis we used the kit QuikChange® II XL from Stratagene®. For the mutagenesis the first and most important step was the design of the special primers that would allow us to cause the specific mutation. In our case the target was to eliminate the seed sequence of the miRNAs from the 3' UTR of PARN. The primers had to fulfill certain criteria such as length of 25-45 base pairs, the mutation has to be in the middle of the sequence, melting temperature ≥75°C and a minimum of 40% of GC content. We addressed successfully all of the prerequisites and the primers that were used are shown below. Notice that each of the miRNAs we test, 29a and 1207, have 2 sites on our 3' UTR that are of interest and so we created a set of primers for the elimination of both of these sites.

**Table 6 Primers for the site-directed mutagenesis. Direction 5'➔3'**

| | |
|---|---|
| 1st position for Δ29a FOR | **GCAGCAAACCGGTCGCTGTGAGCAAGAGC** |
| 1st position for Δ29a REV | **GCTCTTGCTCACAGCGACCGGTTTGCTGC** |
| 2nd position for Δ1207 FOR | **CGGTTGTGCCTCCCACCATAGCTGCC** |
| 2nd position for Δ1207 REV | **GGCAGCTATGGTGGGAGGCACAACCG** |
| 3rd position for Δ29a FOR | **CTGTTCTTATGCGTGTTCACTTTCCAGAG** |
| 3rd position for Δ29a REV | **CTCTGGAAAGTGAACACGCATAAGAACAG** |
| 4th position for Δ1207 FOR | **CGTGCAAATCTACAACATGCATTCTCCG** |
| 4th position for Δ1207 REV | **CGGAGAATGCATGTTGTAGATTTGCACG** |

After the primers we set up the reaction for the mutagenesis according to the provided manual. Once again a table below shows the reagents used and the protocol. The basis of this kit is that the oligonucleotide primers, each complementary to opposite strands of the vector, are extended during temperature cycling by PfuUltra HF DNA polymerase, without primer displacement. Extension of the oligonucleotide primers generates a mutated plasmid containing staggered nicks. Following temperature cycling, the product is treated with Dpn I. The Dpn I endonuclease is specific for methylated and hemi methylated DNA and is used to digest the parental DNA template and to select the mutated plasmid over the template. DNA isolated from almost all E. coli strains is dam methylated and therefore susceptible to Dpn I digestion. The vector that remains incorporates the desired mutations is then transformed into XL10-Gold®*** ultracompetent cells following the same protocol as discussed above. The amount of μl needed each time for DNA and primers was calculated after diluting and measuring with the Nanodrop ND-1000.

| Reagents | Volume 1x | Protocol |
|---|---|---|
| **Reaction Buffer 10x** | 5 µl | 95°C 1 minute |
| **DNA template** | 10 ng | 18 cycles: |
| **Primer FOR** | 125 ng | **95°C 50 seconds** |
| **Primer REV** | 125 ng | **60°C 50 seconds** |
| **dNTP's** | 1 µl | |

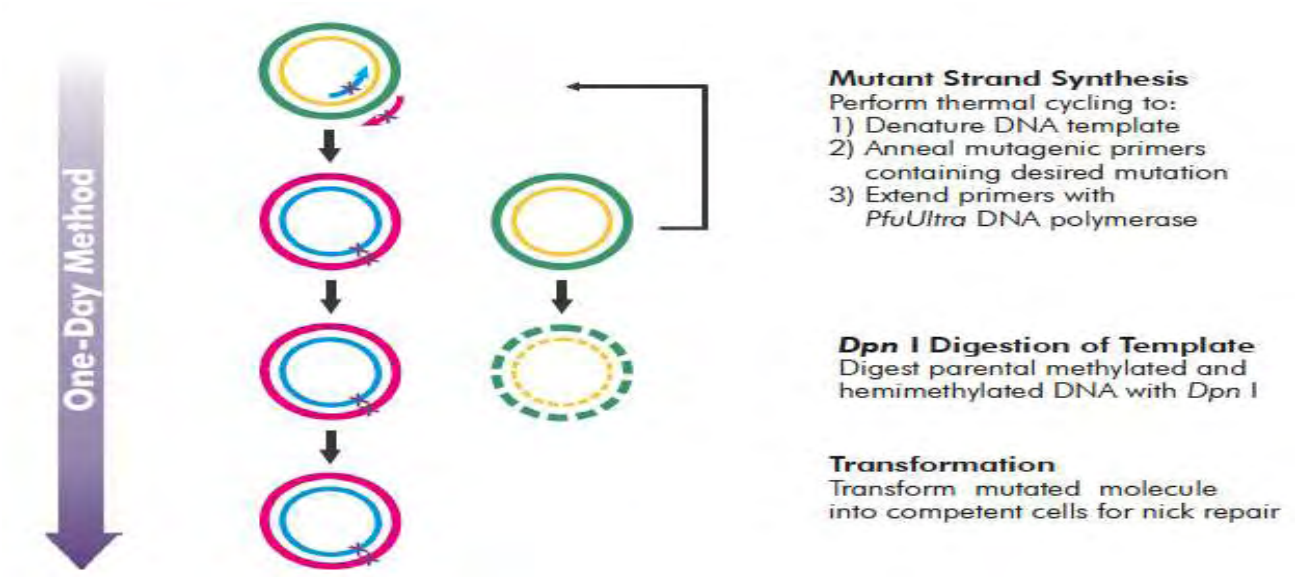


**Figure 10 The principle of the mutagenesis protocol**

**Table 7 Site-directed mutagenesis reaction volumes and protocol**

## 4.7. *Sequencing*

| | |
|---|---|
| **QuikSolution™** | 3 µl |
| **Water** | Until final volume is |

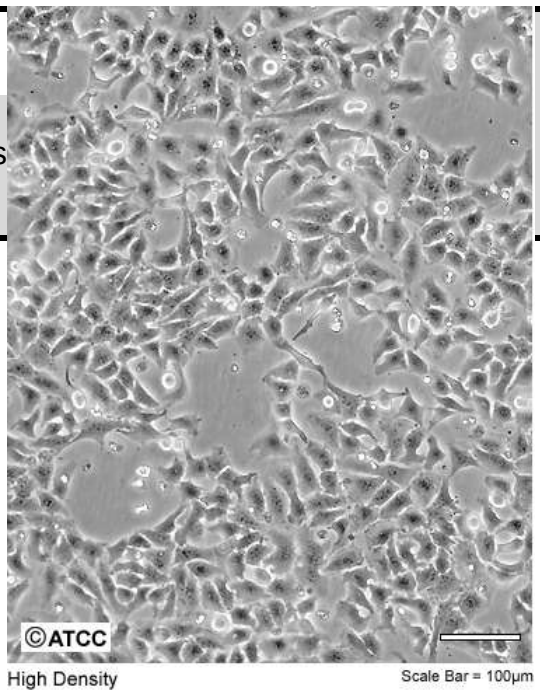


**Figure 11 HeLa cells in high density**

For sequencing of our plasmids we used BMR genomics an official spin-off of the University of Padova. To prepare the samples we used PCR tubes of 0.1ml and add 500ng of our plasmid along with the primer we use each time. For the fist part of this project and the cloning of 3' UTR of PARN we used a special primer that binds to the luc gene of our plasmid right before our area of interest. For the second part of the mutagenesis we checked some of the constructs using this same primer and the rest were checked using another primer that bound approximately half-way along the 3' UTR of PARN. Below you can see the sequences of these two primers.

**Table 8 Primers used for sequencing our cloned fragments from pGLO vector 5'➔3'**

| | |
|---|---|
| LUC2 FOR SEQ | **CATCGCCGTGTAATAAT** |
| PARN1207 5p-29a FOR | **ACTGGAGCTCCATGGGGGATGTACGAGTAA** |

## 4.8. *Cell line*

Our cell line of choice is HeLa. HeLa cells are easy to grow and to transfect. It is a cell line derived from human cervix tumor of a 31 year old black person. Their ability to be immortal is based on the expression of an active telomerase during the cell division stage. They form a monolayer of cells inside the flask that they grow. The conditions in the incubator are 37°C, air 95% and 5% $CO_2$. The base medium for this cell line is Eagle's Minimum Essential Medium (Gibco) with the addition of 1% glutamine, 10% fetal bovine serum and 1% Penicillin Streptomycin (Pen Strep). For long-term storage we use liquid nitrogen vapor phase.

HeLa cells have a doubling time of about 24 hours. Subculturing was done 2 times per week every 3 days. To do this we had to follow these steps:

- Under the microscope we check that the confluence of our flask is above 90%

- Aspirate the medium and wash twice with Phosphate-Buffered Saline (PBS)
- Add 1ml of trypsin (EDTA 1%)
- Place the cells in the incubator and wait for 2 minutes
- Observe that the cells are detached
- Add 9ml of DMEM with glutamine and Pen Strep antibiotic
- Using a pipette of 10ml mix the cells by pipetting up and down to break any clumps
- Put 2ml of your previous cell culture in a new flask containing 16ml of DMEM in a dilution 1:8

### 4.9. *Transfection*

For the transfection of our eukaryotic cells we use the MIRUS TransIT®-LT1 transfection reagent. The protocol requires the use of two solutions. The first solution, from now on solution A, contains the DNA we wish to transfect and opti MEM®. The second solution, from now on solution B, contains opti MEM® and the transfection reagent. This second solution can be common for all the conditions whereas solution A has to be unique for each condition. In our experiments we performed co-transfections of HeLa cells with two plasmids. The one plasmid was the pGLO vector (Promega) where we had cloned our 3' UTR as a whole or in fragments, downstream the Luciferase gene, and the other one was the pSiUx vector that was used in order to over express our miRNAs in the cells. For each condition we used 50ng and 500ng of plasmid respectively per well. For solution A also we calculated the amount of opti MEM® by considering that we needed 30μl of solution A per well. For solution B the amount of opti MEM® was calculated by multiplying by the number of wells the amount of solution B that was needed per well, that is 20μl. In the solution B we also had to add our transfection reagent. The amount of MIRUS required was 3μl of transfection reagent for every 1000ng of DNA used in the co-transfection. When all solutions were prepared we mix them and incubate at room temperature for 20 minutes. Subsequently we add 50μl of the mixture to each well. MIRUS does not require a change of medium like other reagents because it is not toxic to the cells.
For every transfection we tested our conditions on 24 and 48 hours. The amount of cells used in each set of conditions was different. For the 24 hours we used 60000 cells and for

the 48 hours we used 50000 cells. The cells were put in a 24-well plate one day before the transfection so that they could attach to the surface of the plate. In order to have no interference with our results on the Luciferase assay we used DMEM White with 1% glutamine for the transfection.

### 4.10. *RNA extraction*

For the RNA extraction from HeLa cells we used TRIzol® reagent from Life Technologies.

TRIzol® Reagent is a monophasic solution of phenol, guanidine isothiocyanate, and other proprietary components which facilitate the isolation of RNA either large or small molecular size. TRIzol® Reagent maintains the integrity of the RNA due to the inhibition of RNase activity while disrupting cells and dissolving cell components during sample homogenization.

For our protocol we use cells that grow on a 24-well plate. We first remove the medium and clean the well using 500 µl Phosphate Buffer Saline (PBS). We aspirate the PBS and add 50 µl of trypsin 1% EDTA. After an incubation of 2 minutes in the cell incubator the cells are detached from the plate. We then add 450 µl of DMEM with phenol red and glutamine, PenStrep and FBS. We resuspend the cells and transfer them in an eppendorf tube of 1,5 ml. We centrifuge for 10 minutes at 13000 rpm at 4°C to form a pellet. We discard the supernatant and store the pelleted cells at -80°C until the extraction.

For the extraction protocol we add to the pelleted cells 300 µl of TRIzol® under the chemical hood and resuspend the cells. Incubate at room temperature for 5 minutes. Then we add 60 µl of Chloroform also under the chemical hood. We mix using vortex for 15 seconds and incubate for another 5 minutes at room temperature. We then centrifuge for 15 minutes at 12000 rpm 4°C. We carefully take only the upper phase (aqueous) from the tube. We must be careful not to touch the pink TRIzol® phase (organic) and the interphase that contains cell debris. We transfer the chloroform phase in a new tube and and 150 µl of isopropanol to precipitate the RNA. We mix fast using a vortex and incubate for 15 minutes at room temperature. After the incubation we centrifuge once again same speed and

temperature for 10 minutes this time. We carefully remove the supernatant isopropanol and add 300 μl of ethanol 75%. In this step we wash the RNA pellet. Centrifuge again for 5 minutes and remove ethanol from the tube. We allow some time (5-10 minutes) for the pellets of RNA to air dry under the chemical hood while in ice. Finally we resuspend the pellets in 32 μl of double distilled water. We store the extracted RNA in -80°C.

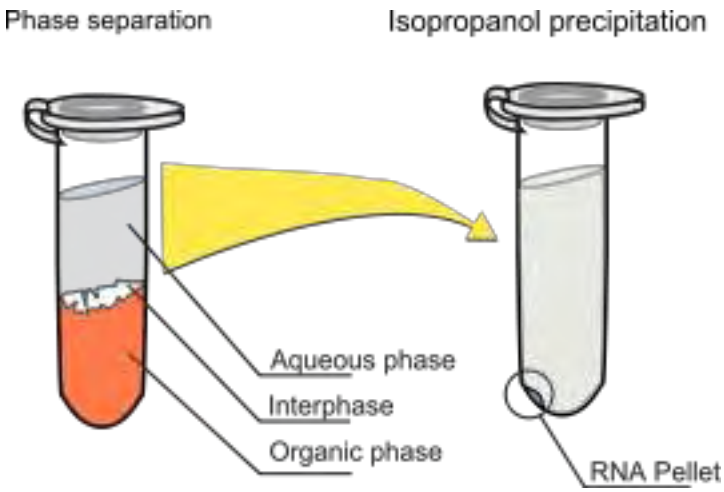


Figure 12 The diphasic solution of TRIzol and chloroform

## 4.11. *qRT-PCR for the detection of miRNAs*

For the quantitative real-time PCR we use the miRCURY LNA™ Universal RT microRNA PCR Exiqon Kit. It is a kit based on the use of SYBR® green. The difference in this kit is that we have a universal reverse transcriptase cDNA synthesis. By universal we mean for all the miRNAs in the cell followed by a real-time PCR for the detection of the miRNAs of interest using as mentioned above SYBR® green.

Table 9 Reverse transcription reaction and volumes

| Reagents | Volume 1x | Protocol |
|---|---|---|
| **5x Reaction Buffer** | 2 μl | 60 minutes at 42°C |
| **Nuclease-free water** | 5 μl | Heat-inactivate reverse transcriptase for 5 minutes at 95°C |
| **Enzyme mix** | 1 μl | |
| **Template RNA (5 ng/μl)** | 2 μl | Cool to 4°C |
| **Total Reaction volume** | 10 μl | |

The first part of the protocol requires the dilution of the RNA samples to a concentration of 5 ng/μl using nuclease free water. We then create a working solution for all of our samples that will be divided in aliquots. The working solution has to remain in ice because it

contains the enzyme. The details about the mix are in the following table. The RNA is added last after the mix has been aliquoted.

We mix the reaction gently and do a spin down and put in the thermocycler.

From the cDNA prepared we perform a dilution of 1:80. We then prepare the real-rime PCR master mix. The reagents are shown in the following table along with the protocol used. Again the master mix is prepared for all the samples and then aliquoted. Only this time because of the specific sets of primers we prepare more than one master mix. Also the cDNA template is added last in the well after we dispense the mix. The real-time is conducted on 384-well plates.

**Table 10 Real-time PCR reaction volumes and protocol**

| Reagents | Volume 1x | Protocol |
|---|---|---|
| **PCR Master mix** | 5 µl | 95°C for 10 minutes |
| **PCR primer mix** | 1 µl | 40 cycles of: |
| **cDNA template** | 4 µl | **95°C 10 seconds** |
| **Total Reaction Volume** | 10 µl | **60°C 1 minute and Melting curve** |

For our calculations we used the 2-ΔΔCt method. This method relies on two assumptions. The first is that the reaction is occurring with 100% efficiency; in other words, with each cycle of PCR, the amount of product doubles. The second assumption of the 2−ΔΔCT method is that there is a gene (or genes) that is expressed at a constant level between the samples. This endogenous control will be used to correct for any difference in sample loading. For each sample, the difference in CT values for the gene of interest and the endogenous control is calculated (the ΔCT). Next, subtraction of the control-condition Δ CT from the treated-condition ΔCT yields the ΔΔCT. The negative value of this subtraction, the −ΔΔCT, is used as the exponent of 2 in the equation and represents the difference in “corrected” number of cycles to threshold. The exponent conversion comes from the fact that the reaction doubles the amount of product per cycle.

1. $\Delta Ct_{(\text{test sample})} = Ct_{(\text{target gene, test sample})} - Ct(_{\text{reference gene, test sample}})$

2. $\Delta Ct_{(\text{control sample})} = Ct_{(\text{target gene, control sample})} - Ct_{(\text{reference gene, control sample})}$

3. $\Delta\Delta Ct = \Delta Ct_{(\text{test})} - \Delta Ct_{(\text{calibrator})}$

Figure 13 Steps of the ΔΔCt method

### 4.12. *Quantification of nucleic acids*

For the quantification of the nucleic acids we used the Nanodrop ND-1000 by Thermo Scientific. The NanoDrop ND-1000 UV-Vis Spectrophotometer enables highly accurate analyses of samples as small as 1μl. It has a full-spectrum UV-Vis absorbance analyses (220-750nm) for measuring absorbance of DNA, RNA, dyes, proteins and microbial cell culture OD. Only 1,5 μl of sample needed for the quantification. It has a large dynamic range: 2-3700 ng/μl of dsDNA. A single measurement takes only 10 seconds.

### 4.13. *Luciferase*

For the Luciferase assay we used the Promega Dual-Glo® Luciferase Assay System. Measures Firefly Luciferase and Renila Luciferase . The normalization of the Firefly with the Renila helps differentiate between specific and non-specific responses as well as the transfection efficiency. The protocol is done using the 24-well plate were the cells grow without the need to detach them and pellet them. We add 35μl of DMEM white with 1% glutamine to well and 35μl of the special Dual-Glo® buffer that contains the substrate for the Firefly Luciferase. We cover the plate because of the photosensitive reagents and shake them for about 20 minutes at room temperature. During this time the reagent will induce lysis of the cells. Immediately after the shaking we put 20μl of the lysate to 384-well plate. Using the TECAN Infinite® 200 we measure the luminescence. Subsequently we add to each well 20μl of the buffer that will serve as the substrate for the Renila. This reagent is made by diluting 100 times the Renila substrate of the commercial kit with the special Dual-Glo® Stop & Glo® Buffer. This reagent is quite sensitive to the light so we immediately cover our plate and incubate at room temperature for 20 minutes. After that time we are able to measure the activity of the Renila using again the TECAN Infinite® 200.

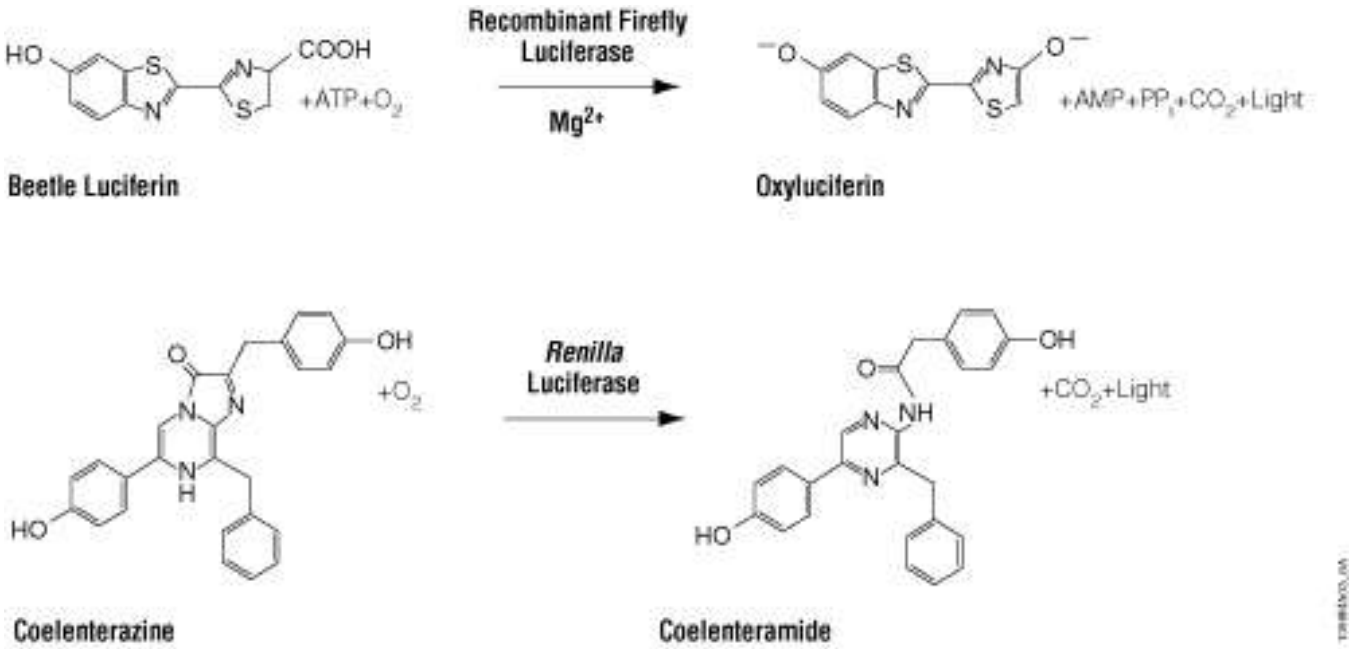


**Figure 14 The reactions of the two Luciferase s**

# 5. Results & Discussion

## 5.1. *Overexpression of miR-29a and miR-1207*

First we validated the overexpression of miR-29a-3p and miR-1207-5p in HeLa cells. Following the protocol mentioned in material and methods we transfected HeLa cells using the miRNA-overexpressing pSiUx vectors provided by the lab. These vectors can produce miRNAs from both strands of the hairpin structure of the pre-miRNA. They can be distinguished by their names that indicate the strand that produces them (3p and 5p respectively). Therefore, we decided to use a qRT-PCR enabling us to monitor the overexpression of the miRNAs produced from both both the 5p and the 3p. The following figures (15-22) provide a graphic representation of our data.

In most cases we were able to verify the overexpression with statistically significant results. As a control we used HeLa cells transfected with the empty vector, this means that the there is no genomic region for a miRNA cloned inside the vector. In particular, miR-29a seems to be overexpressed compared to our control. In most cases the overexpression of miR-29a is not gigantic mainly because our cell line (HeLa) already express a very good basal level of this miRNA. Therefore it is not possible to obtain a bigger overexpression. The levels of miR-29a are around 1.2 to 1.9 fold change during the 24 and 48 hours with the exception of miR-29a-5p that during 48 hours it has a fold change of 10. Our attention was drawn to the fact that miR-29a seems also to be overexpressed when we introduce the vector for the overexpression of miR-1207. To our knowledge this is probably because of some compensatory or defensive mechanism of the cells against the stress cause by the transfection process. The same thing happens with the overexpression of miR-29a where we observe an overexpression of miR-1207 especially the 3p.

In general the transfection of miR-1207 achieved very good levels both in 24 and 48 hours with a minimum of 3.9 fold change to a maximum of 31. The most noticeable overexpression levels is achieved by miR-1207-3p where we see a very significant fold change of more than 30 in the first 24 hours.

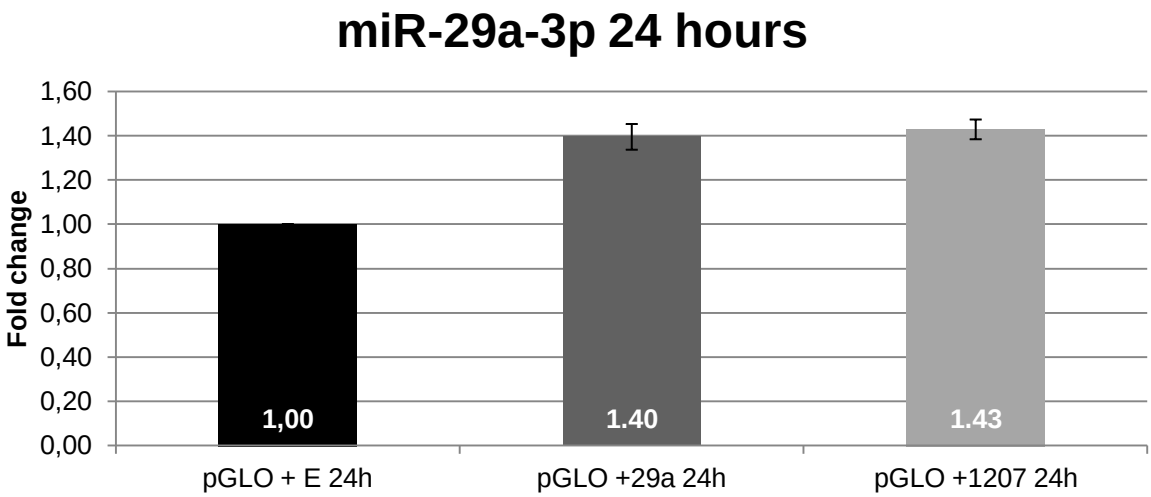


**Figure 15 Fold change in the expression levels 24 hours after transfection of HeLa cells with the overexpressing vector for the miR-29a. P-value was calculated using one-tailed unpaired t-test with equal variance. One star indicates P-value ≤ 0.05, two stars is ≤ 0.01.**

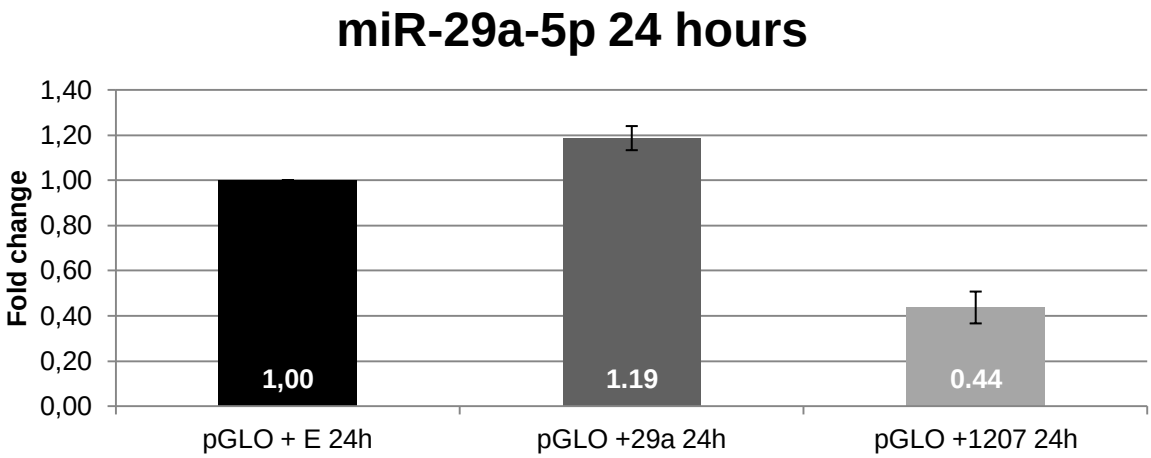


**Figure 16 Fold change in the expression levels of miR-29a-5p 24 hours after transfection of HeLa cells with the overexpressing vector for the miR-29a.**

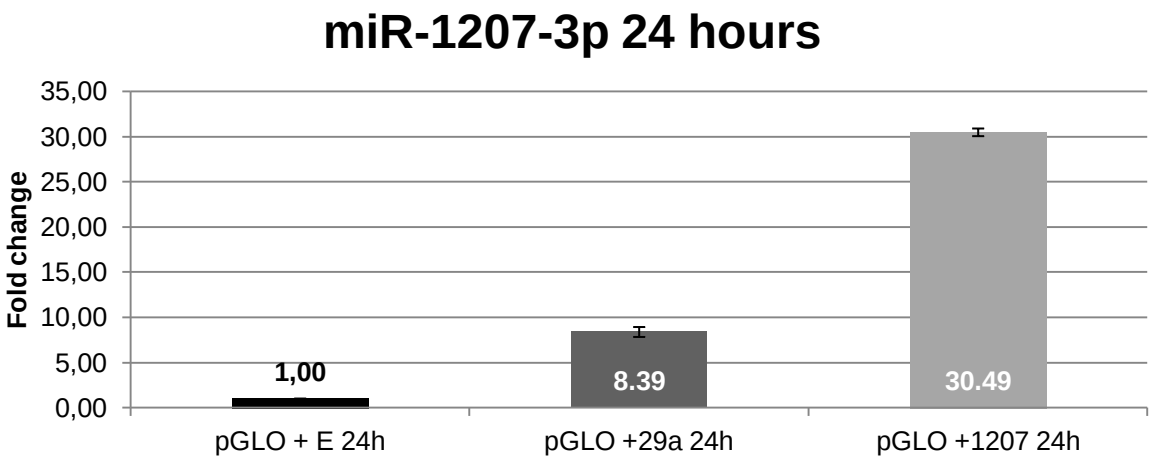


**Figure 17 Fold change in the expression levels of miR-1207-3p 24 hours after transfection of HeLa cells with the overexpressing vector for the miR-1207.**

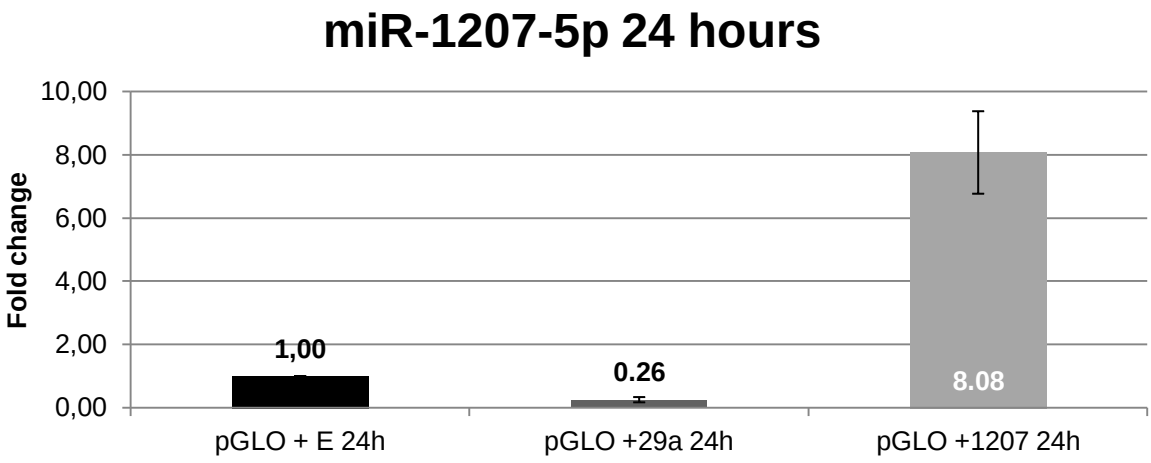


**Figure 18 Fold change in the expression levels of miR-1207-5p 24 hours after transfection of HeLa cells with the overexpressing vector for the miR-1207.**

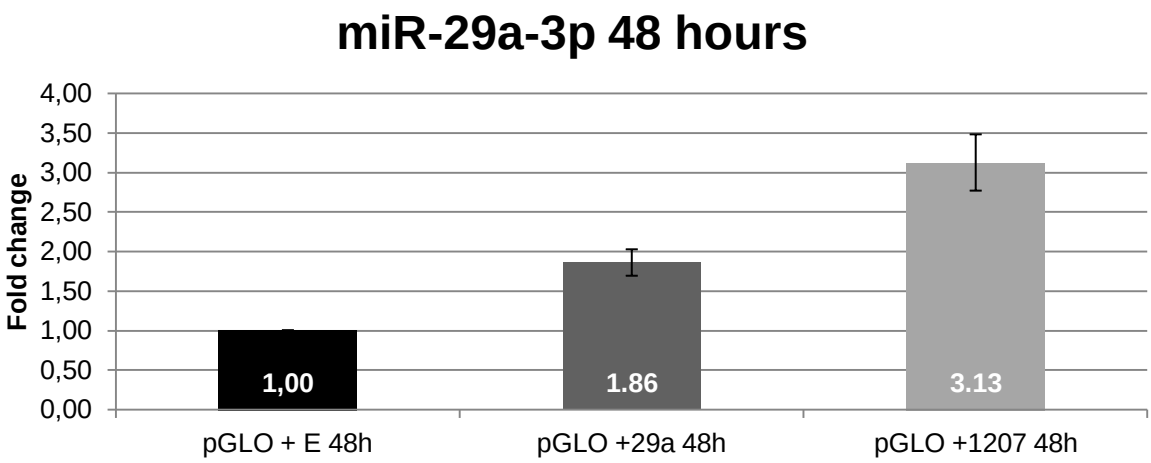


**Figure 19 Fold change in the expression levels of miR-1207-3p 24 hours after transfection of HeLa cells with the overexpressing vector for the miR-1207.**

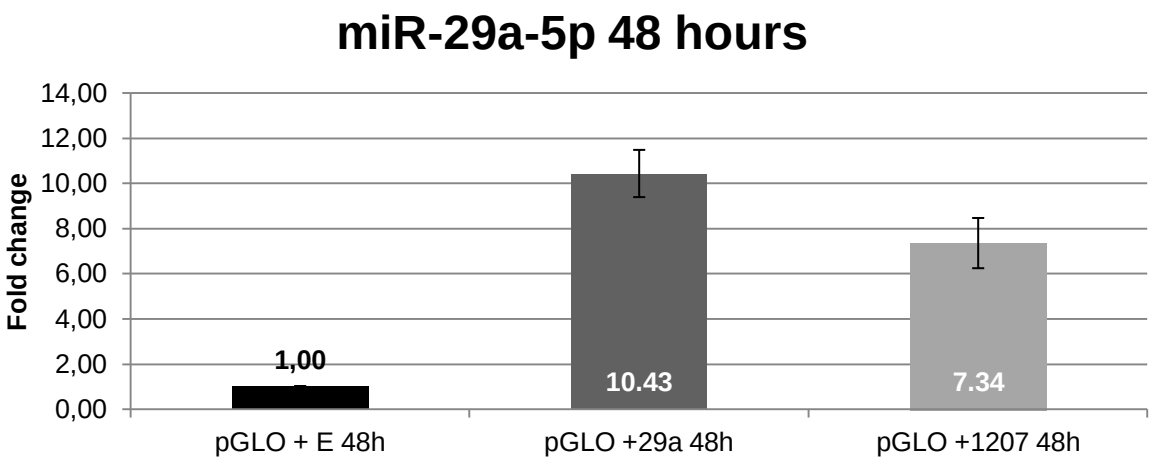


**Figure 20 Fold change in the expression levels of miR-1207-3p 24 hours after transfection of HeLa cells with the overexpressing vector for the miR-1207.**

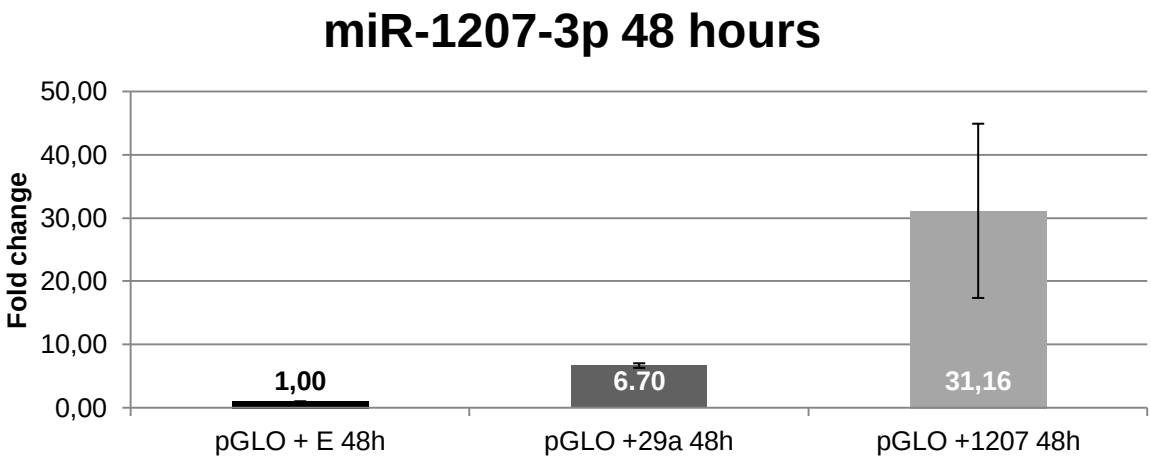


**Figure 21 Fold change in the expression levels of miR-1207-3p 24 hours after transfection of HeLa cells with the overexpressing vector for the miR-1207.**

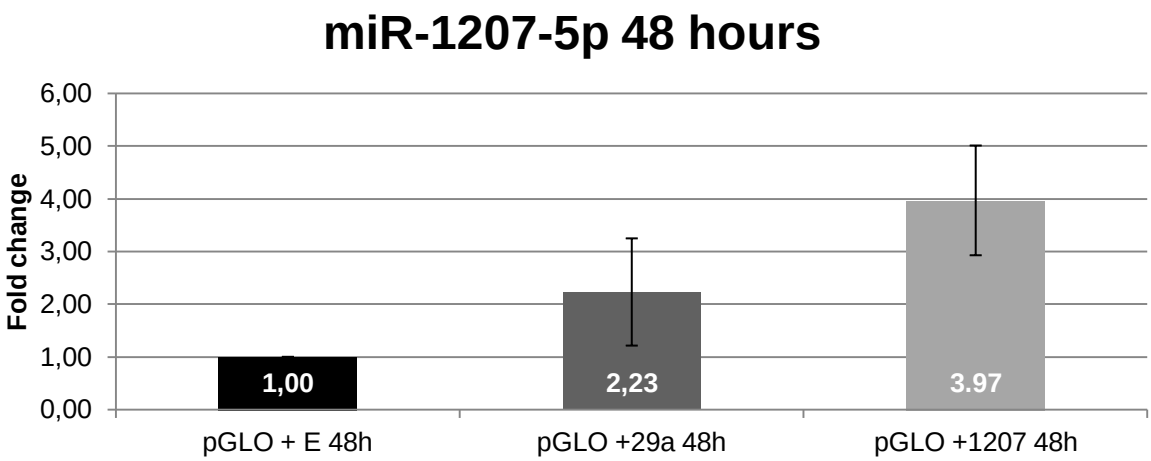


**Figure 22 Fold change in the expression levels of miR-1207-3p 24 hours after transfection of HeLa cells with the overexpressing vector for the miR-1207.**

As a result we can say that our system worked as far as the overexpression of the miRNA is concerned. This enabled us to proceed further with our experiments.

## 5.2. *PARN 3' UTR cloning*

For the purposes of our project we decided to clone the 3' UTR of PARN and fragments of it in the pmirGLO vector. Through this vector we would be able to measure the levels of the Luciferase activity and understand if there is any interaction between the 3' UTR and our miRNAs. For this purpose we designed specific primers, as shown in the materials and methods section, for the amplification of the region from genomic DNA. As mentioned we also created smaller fragments of our 3' UTR. In the first fragment there is one site for the miR-29a-3p, in the second fragment there is a site for miR-1207-5p and in the last

fragment there are two sites, one for each of our miRNA. These last two sites could not be separated because of their proximity so we decided to keep them together in one fragment. This way we were able to check the predictions of the PITA algorithm for each site as to the most efficient binding.

Using the primers we amplified each of our fragments and the whole 3' UTR and restricted it with specific restriction enzymes. The sites for these enzymes were chosen and integrated in our primers so that after digestion we would be able to ligate our PCR product with our vector in a given direction.

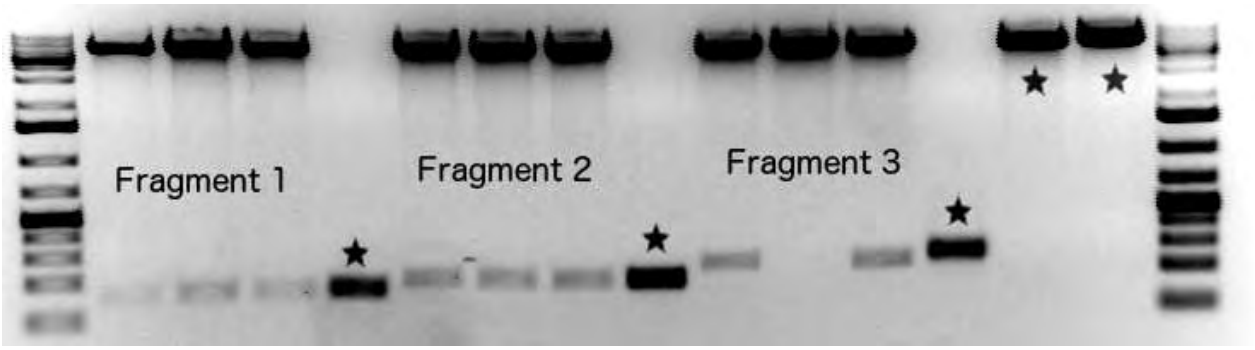


**Figure 23 Results of the cloning for the 3 smaller fragments of the 3'UTR of PARN. In the first three rows we have plasmids obtained by different colonies in the same plate for fragment 1. The fourth row is the control of the band we expect to see and is marked by a star. The same pattern is repeated for the next two fragments. The last two rows contain the plasmid without anything cloned as a control for the size of the plasmid in our samples.**

After the ligation we transformed DH5α cells and allowed them to grow overnight at 37°C on ampicillin plates for the selection. From these colonies we extracted the plasmid DNA and then digested some of it with our chosen restriction enzymes, XhoI and SacI HF®. The result of the digestion is loaded into a 1,5% agarose gel. In figure 23 you see the result of our cloning for the 3 smaller fragments of the 3' UTR of PARN. Signed with the small black stars are the controls. After every three samples you see a control of the fragment we expect and in the last two wells we see the vector digested and non-digested respectively. From the image we see that the cloning probably is correct because the size of the bands appear to be correct. To validate our result we sent the two of the three samples of each fragment for sequencing. From the result of the sequencing we were able to validate the success of our cloning for all of the three fragments.

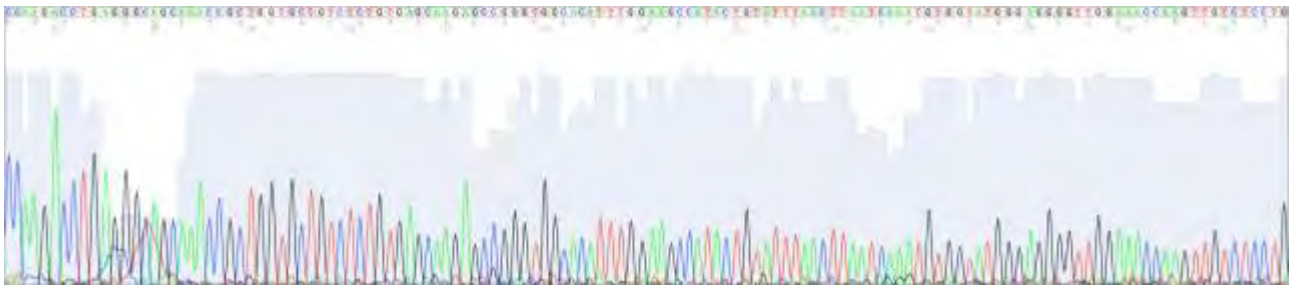

Figure 24 The chromatograph of the cloning of the first fragment that contains the site for miR-29a

The same procedure was followed for the whole 3' UTR of PARN. Again the result are visible on a 1,5% agarose gel. For the validation of the cloning success we again sequenced our products. In figure 26 you can see part of the chromatograph of the total 3' UTR of PARN. Bioinformatic analysis of the sequence allowed us to confirm the results of the cloning. Again the star indicates the band that acts as a control for the band that we want to see cloned in our vector

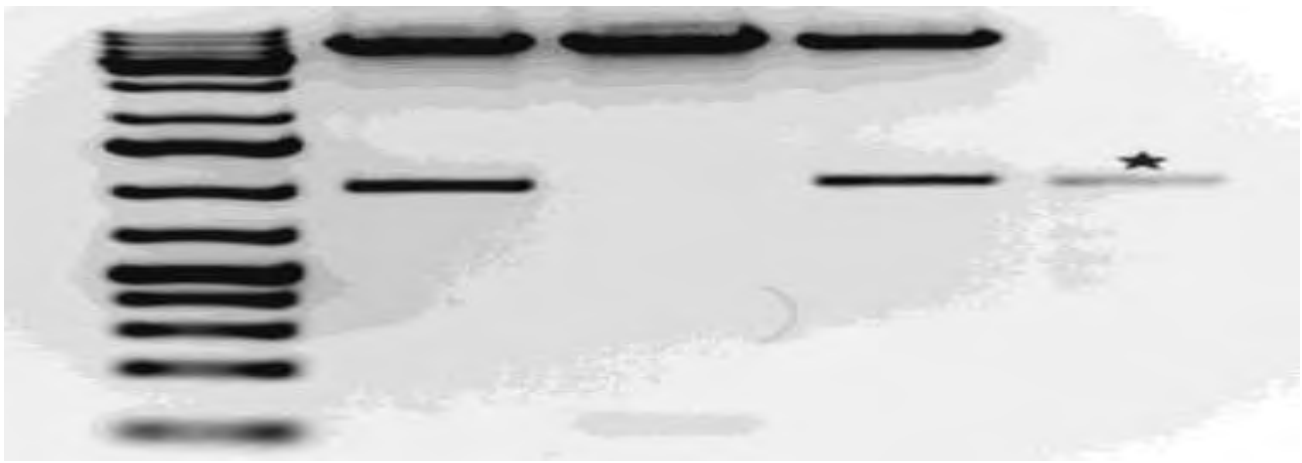

Figure 25 The results from the result of the restriction for the whole 3' UTR. The gel is 1,5 % agarose gel with EtBr. Marked by a star you can see the expected band.

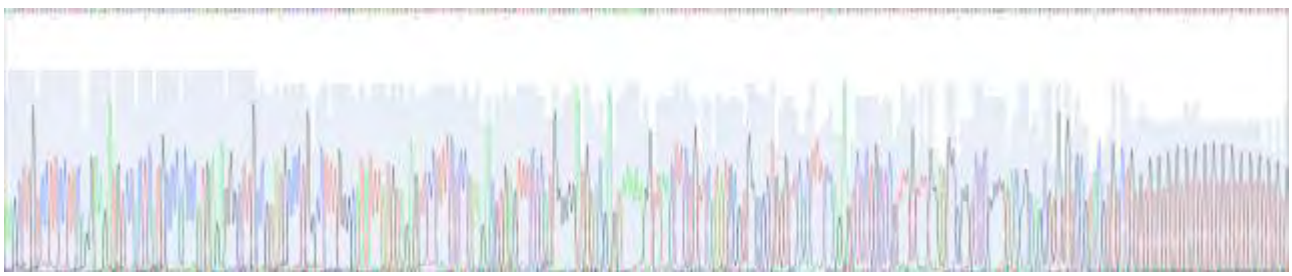

Figure 26 Part of the chromatograph of the PARN 3' UTR.

## 5.3. *Production of mutants for the 3' UTR of PARN*

After the successful cloning of the 3' UTR we decided to proceed also with the creation of mutants. These mutants would allow us to show that whatever effect we observe through the Luciferase assay can be inverted if we eliminate the sites for our miRNA. For this

reason we created mutants of the whole 3' UTR for every one of the four sites that exist on our region. We also created double mutants in which we eliminated two of the sites each time. More specifically the two sites for miR-29a-3p or the two sites for miR-1207-5p. As discussed in materials and methods used specific primers for the mutagenesis.

The results were shown using the same workflow as in cloning. First we transformed our cells, in this case XL-10, and allowed them to grow overnight on ampicillin plates for selection. The plasmid DNA was extracted and then digested with the enzymes of choice. The results were observed on a 1,5% agarose gel and then validated by sequencing. In the gel the recognition of the correct band was done only by the size indicated by the marker. As template for the creation of the double mutants we used the single mutants that we created in the first mutagenesis.

The mutants were created using as template the total 3' UTR and not the smaller fragments. This was the better choice because the size of the fragments is too small around 200 base pairs and the deletion of 8 base pairs seemed as a big intervention. The other fact is that the total 3' UTR has a secondary structure that resembles more to the natural and would not be seriously affected by the deletion. In figures 27 and 28 we see the results from the electrophoresis of the digested mutant plasmids.

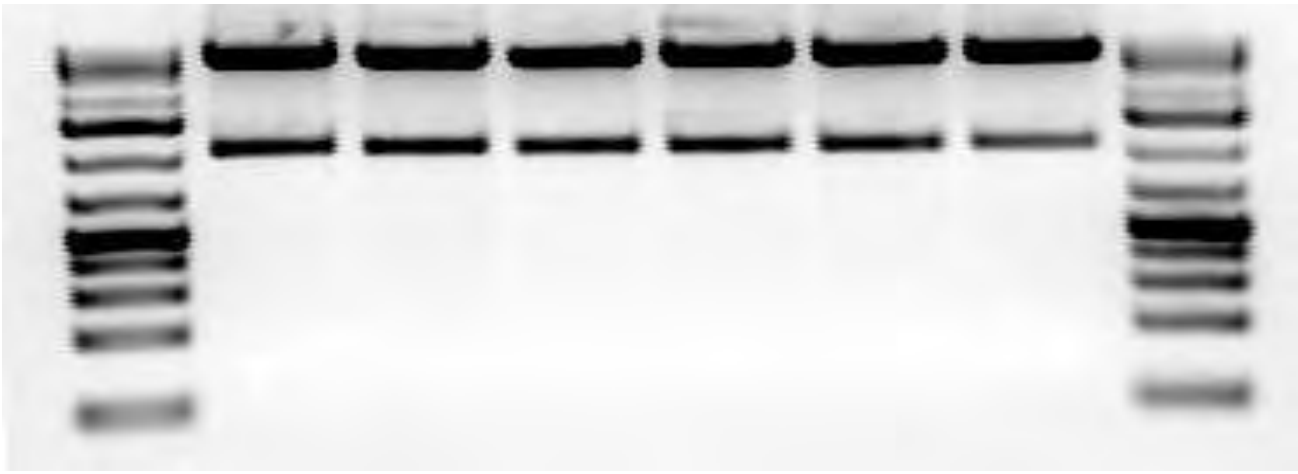

**Figure 27 Gel results for the mutagenesis of a single site. The gel is 1,5 % agarose gel with EtBr. There is no specific control other by the size of the band that is about 1000 bp.**

**Figure 28 Gel results from the mutagenesis of the double mutants. Mutagenesis did not work in the first well. The gel is 1,5 % agarose gel with EtBr. There is no specific control other by the size of the band that is about 1000 bp.**

## 5.4. *Luciferase assay for the investigation of putative interaction between the 3' UTR of PARN and miR-29a or miR-1207*

First we performed a Luciferase assay without introducing any part of the 3' UTR of PARN cloned in our vectors. This way we checked if the overexpression of the miRNAs would cause any problems to the levels of the Luciferase due to possible interactions between the miRNAs and the endogenous PARN in HeLa. Our interest was focused on putative interactions of the endogenous PARN with the miRNA that could interfere in our Luciferase signal. These interactions could lead to the down regulation of the endogenous PARN and cause problems in the stability of the mRNA transcribed by the Luciferase vector, due to improper deadenylation of the transcript. The graph below shows that the minor decreases, 6-11 %, we observed were of no statistical significance. We therefore do not have to take into account any interference of the endogenous PARN with our miRNAs.

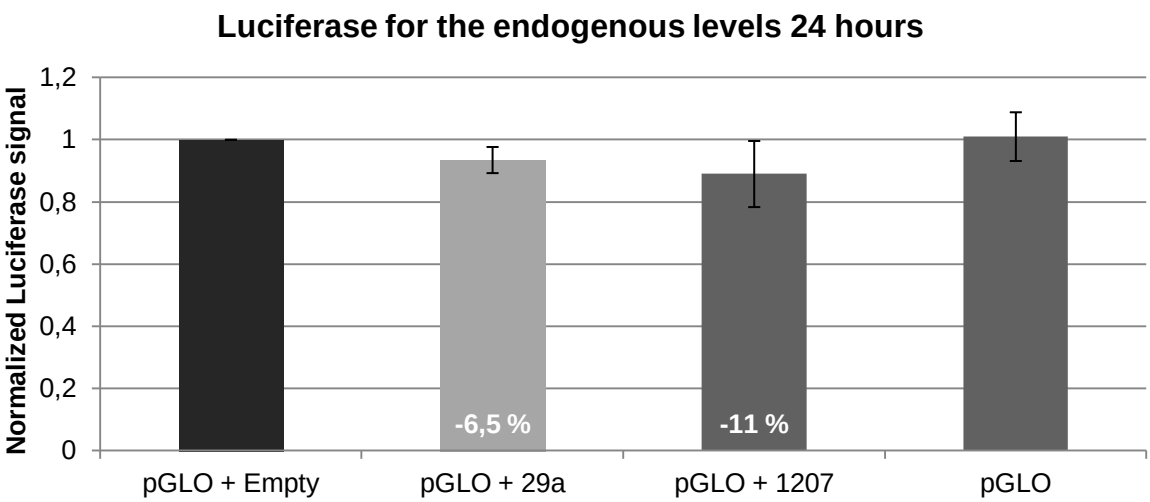


**Figure 29 Luciferase assay results for the experiment used to see if the levels of the Luciferase are affected by the overexpression of our miRNAs in the endogenous condition. P-value was calculated using one-tailed unpaired t-test for samples with unequal variance. Results are derived from three biological replicates.**

Then we performed our assays using our vectors with the cloned fragments. We performed the assay using vectors in which we cloned either one of the fragments or the whole 3' UTR and vectors containing the mutants we created. In each set of data we have HeLa cells that were co-transfected with the Luciferase vector with our testing region and a vector that overexpresses no miRNA, there is another set of cells that has been transfected with the overexpressing vector for the one of our miRNA of interest and finally cells that overexpress miR-608 which is not predicted to bind on our 3' UTR and is used as a negative control. Finally all of our data have been normalized against Renilla Luciferase and against the negative control (miR-608). Below we present the results of the Luciferase assays for the fragments, the whole 3' UTR and the mutants.

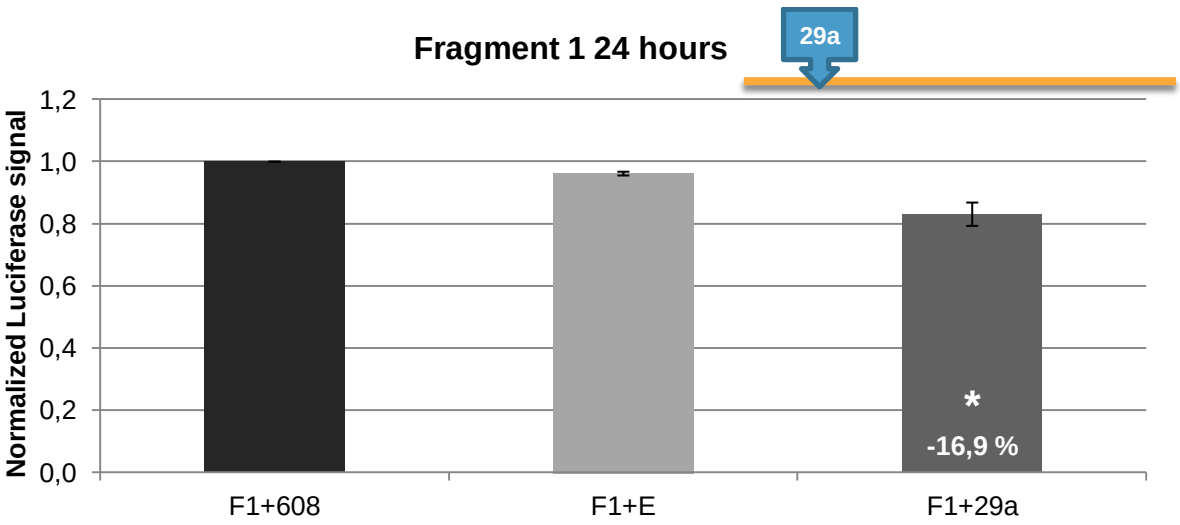


**Figure 30 Luciferase assay result for the first fragment normalized against the negative control. P-value was calculated using one-tailed unpaired t-test for samples with unequal variance. One star indicates P-value ≤ 0.05. Results are derived from three biological replicates.**

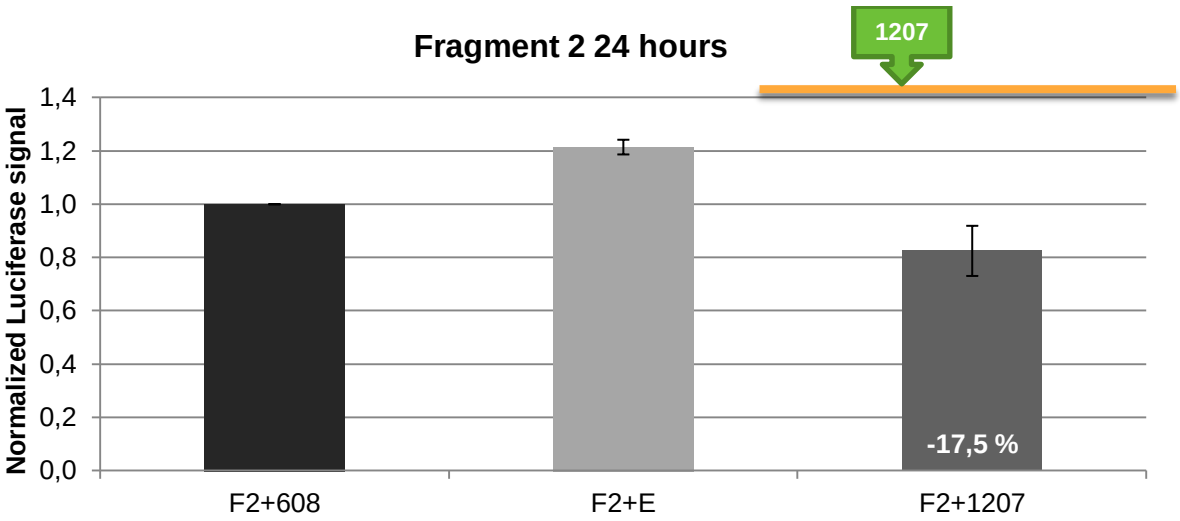


Figure 31 Luciferase assay results for the second fragment compared to the negative control. P-value was calculated using one-tailed unpaired t-test for samples with unequal variance. Results are derived from three biological replicates.

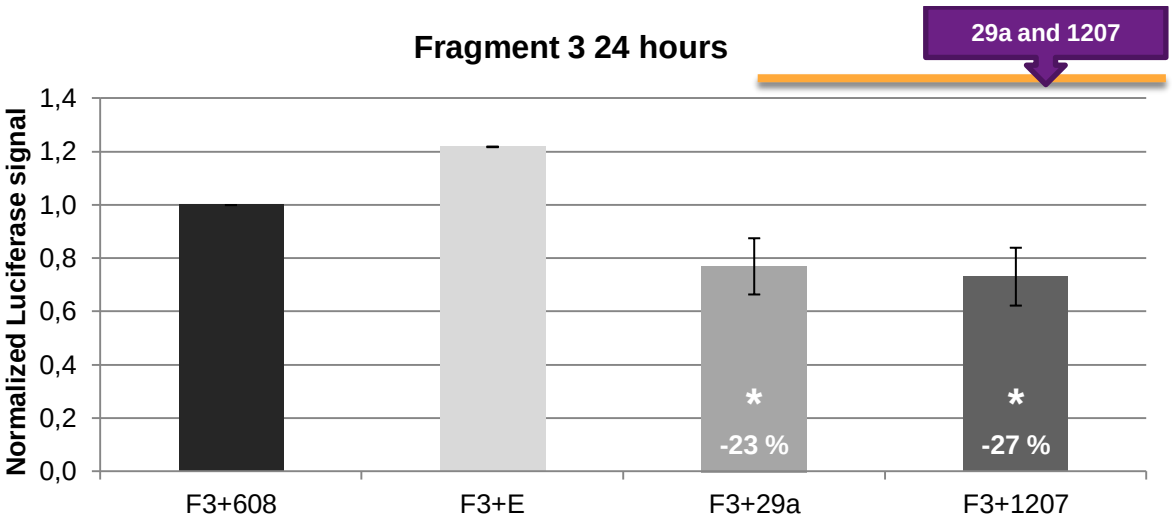


Figure 32 Luciferase assay results for the third fragment compared to the negative control. P-value was calculated using one-tailed unpaired t-test for samples with unequal variance. One star indicates P-value ≤ 0.05. Results are derived from three biological replicates.

Figures 30 to 32 show the graphic representation of our results 24 hours post transfection. We were able to observe a reduction in all fragments but only in two of them, fragment 1 and 3, this reduction was statistically significant. For all the analysis of the Luciferase our main comparison is done between the effect of our miRNAs and the effect of miR-608. We made this choice because this condition seemed more close to a control since in both cases the cells have a miRNA overexpressed. On the contrary in the case of the use of the empty vector for the overexpression of miRNAs we believed that the stress of the cells is not equal to our case.

In particular for fragment 1 we have a reduction of 16,9 % compared to our negative control. In fragment 2 we see a reduction of 17,5 % but it is not statistically significant. Probably this could be a condition that could be repeated to validate further the results. In

fragment 3 we observe the biggest reduction of all the fragments. Since in fragment 3 we have one position for each miRNA we tested it against both. With miR-29a we achieved a reduction of 23 % and with miR-1207 the effect was a bit stronger (27 %). This result drew our attention because the bioinformatic analysis predicted that the sites in fragments 1 and 2 were the most prominent sites to induce an effect (minimum free energy of -24,1 kcal/mol and -36,6 kcal/mol compared to -17,4 kcal/mol and -27,8 kcal/mol respectively). For us this was not the case since the biggest effect was on fragment 3 which contained the two least prominent sites. One reason behind it could be the fact that this fragment has two sites and not only one like the others and maybe the effect is somehow doubled. Also we have observed that the transfection of miR-1207 induces also the overexpression of miR-29a3p and a repression of miR-29a-5p, and, vice versa, transfection of miR-29 induces also the overexpression of mir-1207-3p and a downregulation of miR-1207-5p, so probably we have a combined effect induced from both miRNAs in this case.

Our case about the most prominent sites seems to be established we incorporated the data from the Luciferase assay done for the 48 hours.

The effect seen on the 24-hour experiment for fragments 1 and 2 was lost at 48 hours (figures 33-34): there was no significant decrease for both of the fragments. To our knowledge the 48-hour time is not considered so informative. This is because 48 hours of miRNA overexpression can cause many changes in the cells, so it is difficult to distinguish the specific events. In fragment 3 we noticed that the reduction observed by the overexpression of miR-29a again is lifted like in the other fragments. On the contrary the effect observed by miR-1207 is still observed (reduction of 21 %) and even though it is not significant it is close to the levels of significance compared to the others (figure 35). The reason behind this could be again the fact that the overexpression of miR-1207 causes the overexpression of miR-29a in HeLa. In this way the effect is more persistent because we have the presence of both miRNAs and the fragment has sites for both of them allowing probably a synergistic effect. Of course further investigation and validation is needed for this hypothesis.

Subsequently we decided to examine the 3’ UTR of PARN as a whole. For this reason we used Luciferase vectors with the total 3’ UTR cloned. This way we were able to use a system that resembles to the natural one. The total 3’ UTR adopted secondary structure that is definitely more close to the natural structure compared to our fragments, which

were only a couple hundred base pairs in length. The results are depicted in figures 36 and 37.

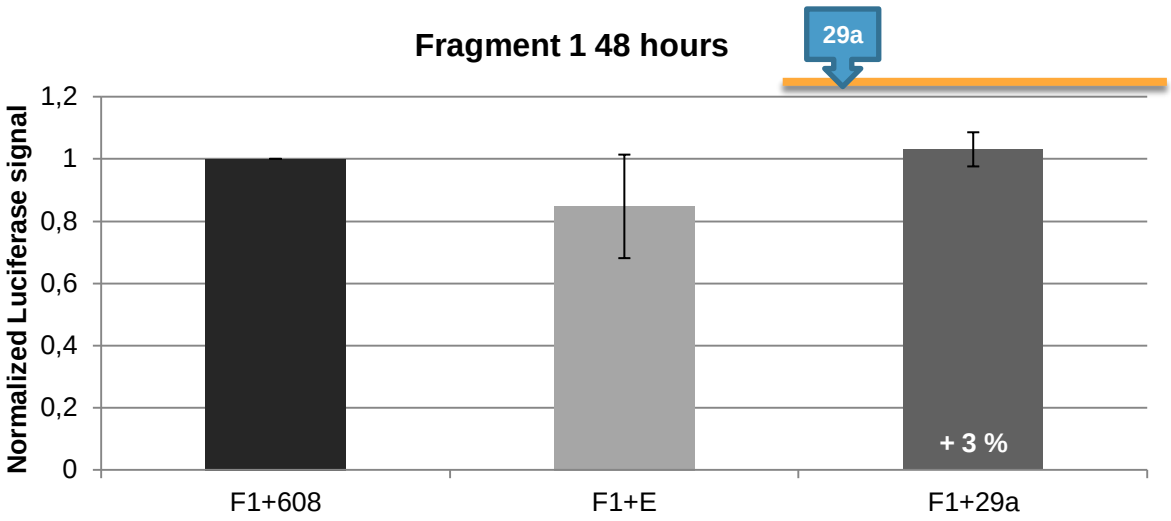


**Figure 33 Luciferase assay results for the 48 hours compared to the negative control. P-value was calculated using unpaired t-test with one tail for samples with unequal variance. Results are derived from three biological replicates.**

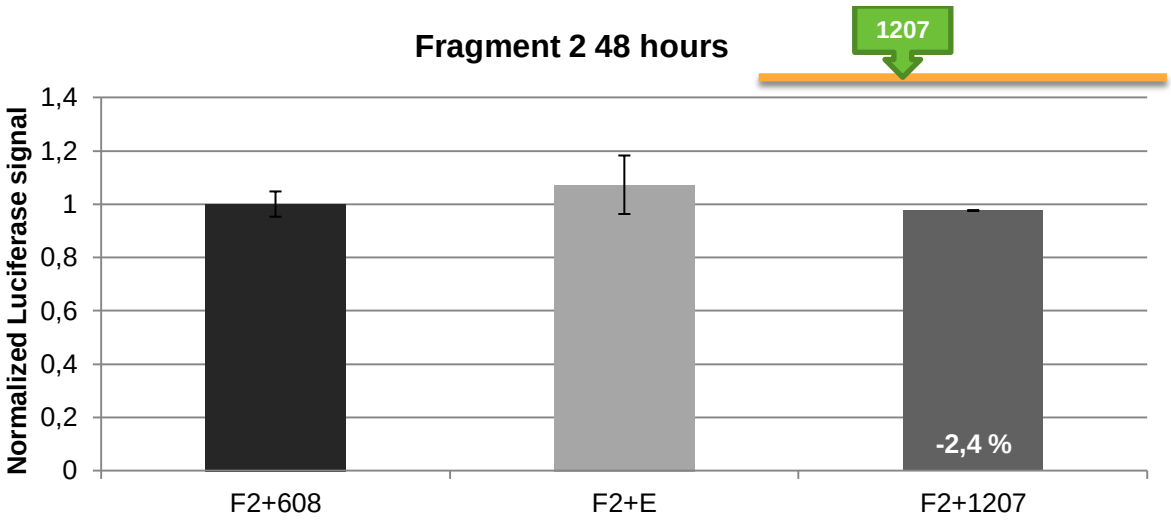


**Figure 34 Luciferase assay results for the 48 hours compared to the negative control. P-value was calculated using unpaired t-test with one tail for samples with unequal variance. Results are derived from three biological replicates.**

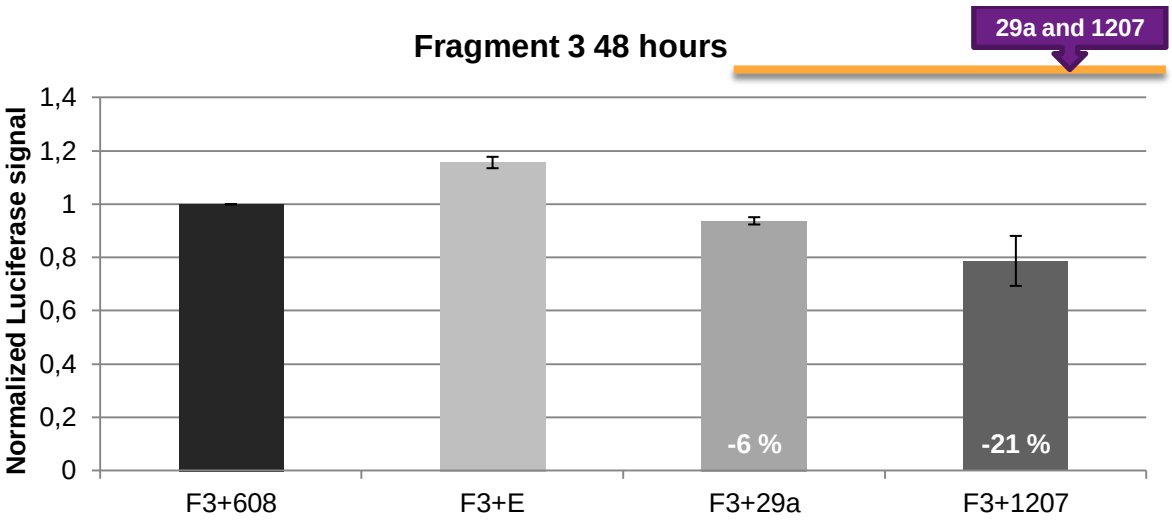


Figure 35 Luciferase assay results for the 48 hours compared to the negative control. P-value was calculated using unpaired t-test with one tail for samples with unequal variance. Results are derived from three biological replicates.

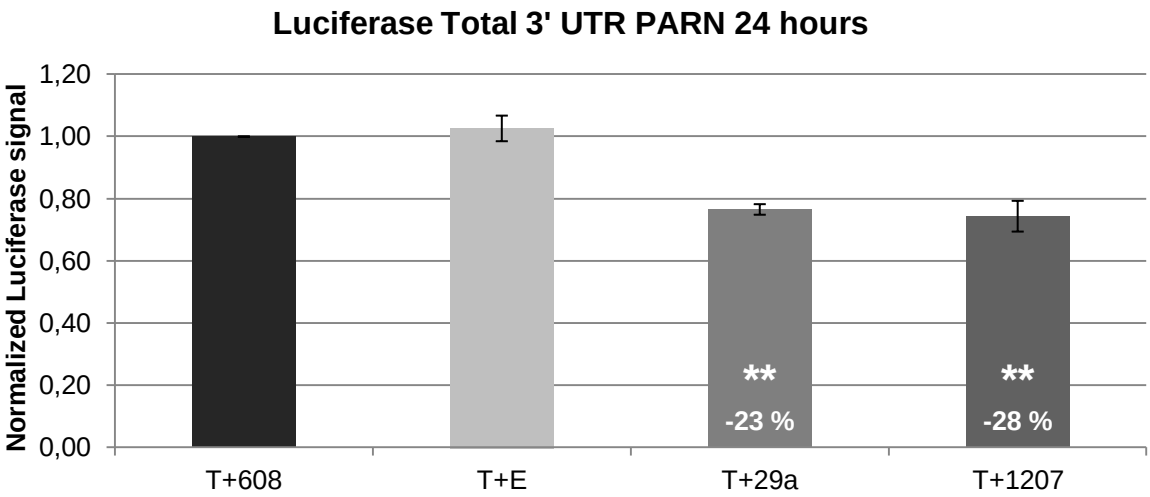


Figure 36 Luciferase assay results for the 24 hours for the whole 3' UTR of PARN. P-value was calculated using unpaired t-test with one tail for samples with unequal variance. Two stars indicates P-value ≤ 0.01. Results are derived from three biological replicates.

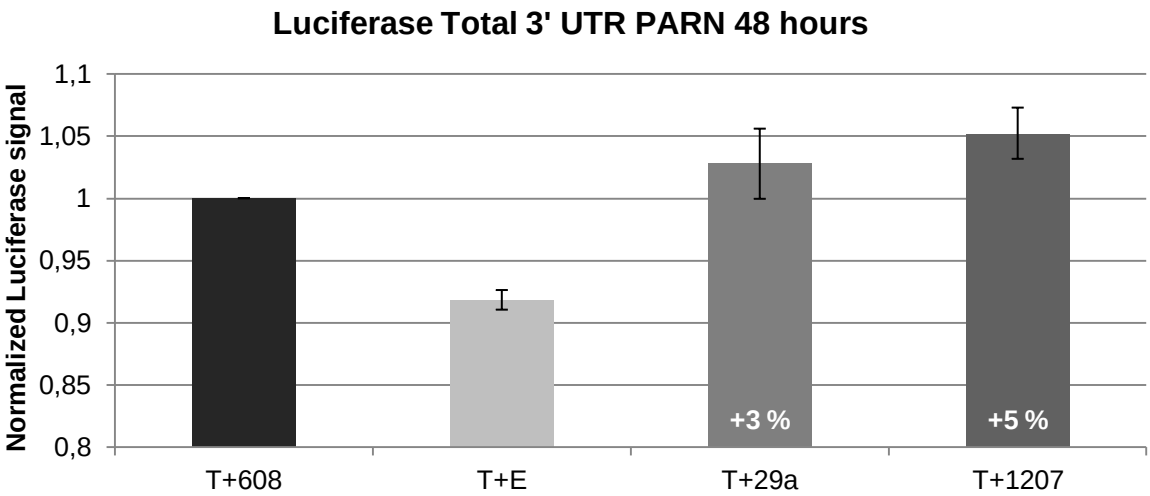


Figure 37 Luciferase assay results for the 48 hours for the whole 3' UTR of PARN. Results are derived from three biological replicates.

As depicted in figure 36, 24 hours post transfection we were able to obtain a strong reduction of more that 20 % with both miRNAs. In particular miR-29a caused a reduction of 23 % and miR-1207 one of 28 %. Even though the difference is small the stronger effect of miR-1207 could be because of the phenomenon we discussed earlier about the overexpression of this specific miRNA. When looking to the results from the 48 hours we noticed that the effect was lifted once again much like the results from the fragments. Again of course we must take into account that the 48 hour time point is enough to cause changes in the cell that lead to the lift of our effect in an non specific way.

For that reason we decided to move one step further and produce mutants of the 3' UTR.

That way we could validate that the reduction we were able to see was not by chance but was due to the binding of the miRNAs. The reason we chose the whole one and not the fragments is simple. First of all, we wanted to allow the adoption of the closest to the natural secondary structure. Moreover the fragments are very small and the deletion of 8nucleotides was not possible for us because it would reduce further their already small size. For that way all of the mutants are derived from the whole 3' UTR.

In figures 38 to 41 we compare wild type 3' UTR to the single mutants we created for each of the four positions. In each graph we se the percentage of change between the wild type and the mutants and the statistical significance of this difference.

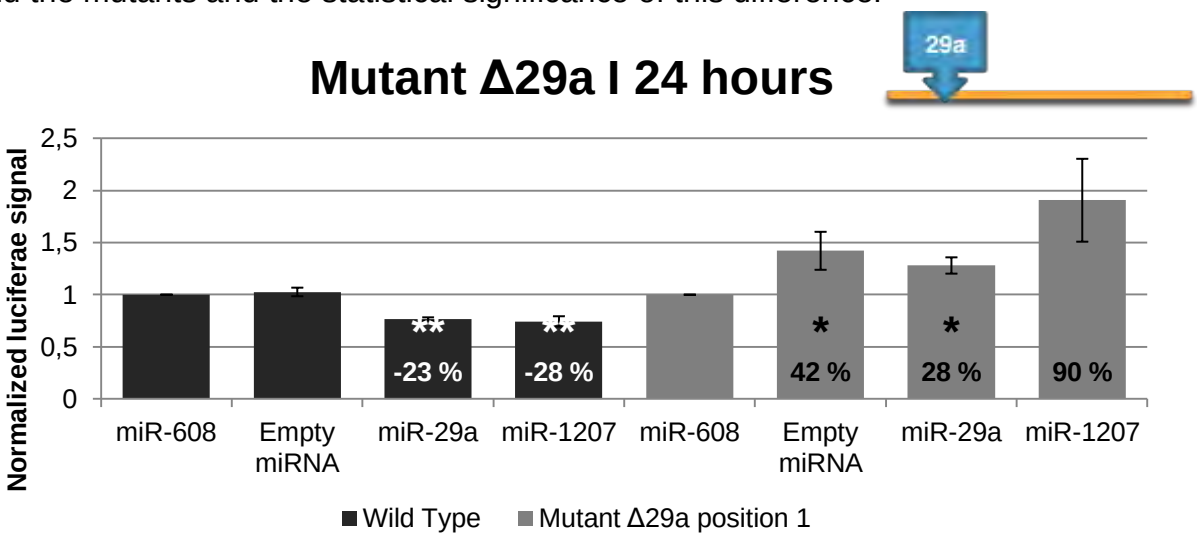


**Figure 38 Comparison of the Luciferase assay results between the wild type 3' UTR and the mutant for the 1st site of miR-29a. In every comparison we see the percentage of difference between the negative control and the different conditions. P-value was calculated using unpaired t-test with one tail for samples with unequal variance. One star indicates P-value ≤ 0.05 two stars indicates P-value ≤ 0.01. Results are derived from three biological replicates for each (wild type and mutant).**

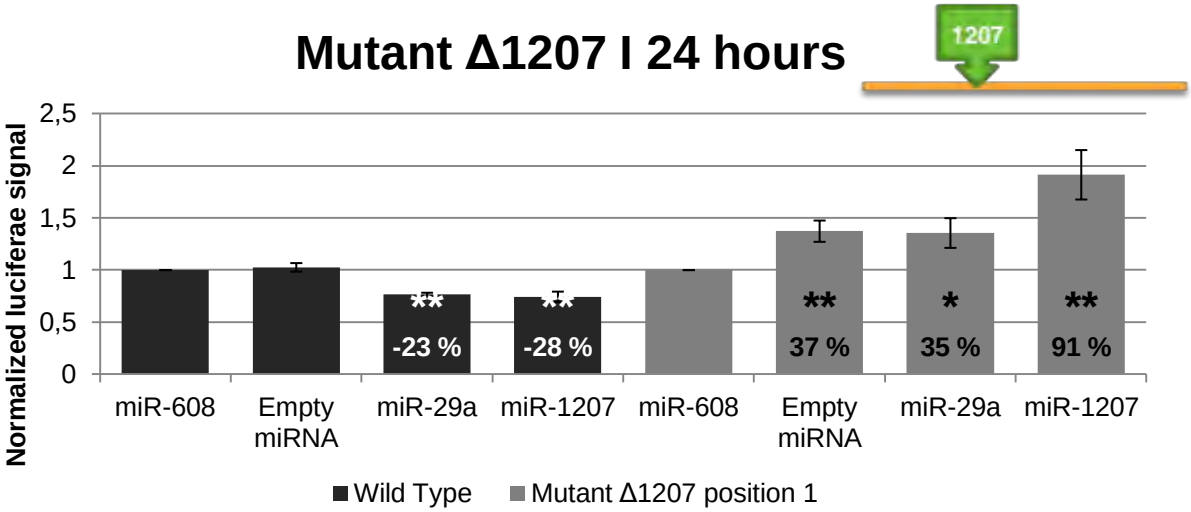


**Figure 39 Comparison of the Luciferase assay results between the wild type 3' UTR and the mutant for the 1st site of miR-1207. In every comparison we see the percentage of difference between the negative control and the different conditions. P-value was calculated using unpaired t-test with one tail for samples with unequal variance. One star indicates P-value ≤ 0.05. Results are derived from three biological replicates for each (wild type and mutant).**

In the graphs we can see the obvious lift of the effect of the wild type by the mutants. The decrease seems to be completely gone in most of the cases. It is worth mentioning however the fact that the decrease is lifted no mater what miRNA we overexpress with our mutants. This is strange as we expected that each mutant would probably resist only to the targeted miRNA. One possibility would be the repetition of this mutant experiment in order to validate even further the results and understand if this effect we see here is actually true. In every case we do not present the data of the 48-hour experiment with the mutants since there was no indication of any effect of the miRNAs on the wild type. For the first two mutation positions (Figure 38 & 39) we have no reduction but instead we have an increase. This is not expected and further experimentation is required to validate our results. For the mutations on the two other sites (Figures 40 & 41) we have better results. The changes in the Luciferase levels are no significant and very small compared to those observed with the wild type constructs.

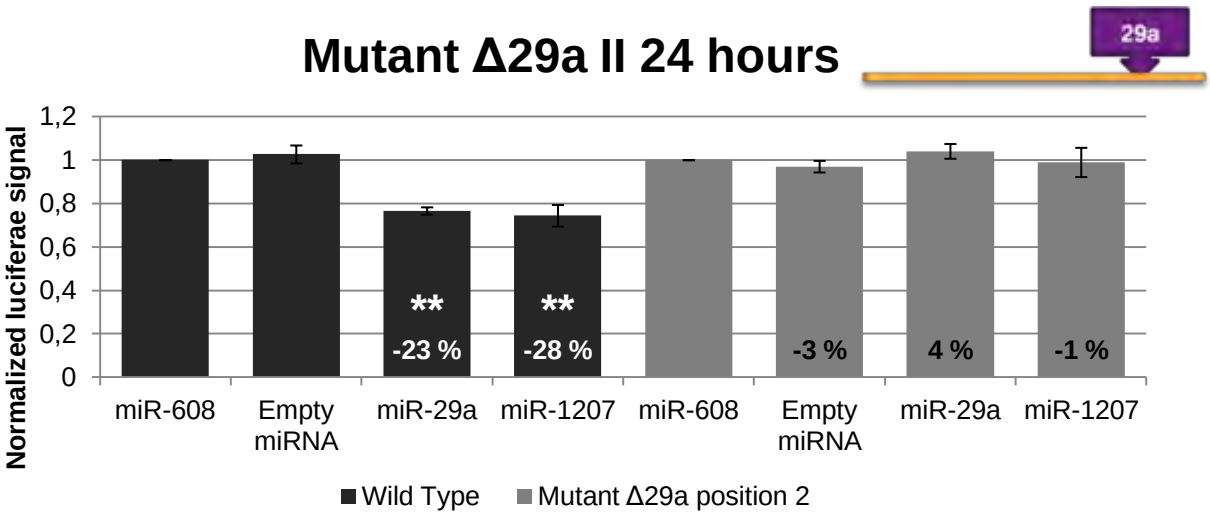


**Figure 40 Comparison of the Luciferase assay results between the wild type 3' UTR and the mutant for the 2nd site of miR-29a. In every comparison we see the percentage of difference between the negative control and the different conditions. P-value was calculated using unpaired t-test with one tail for samples with unequal variance. One star indicates P-value ≤ 0.05 two stars indicates P-value ≤ 0.01. Results are derived from three biological replicates for each (wild type and mutant).**

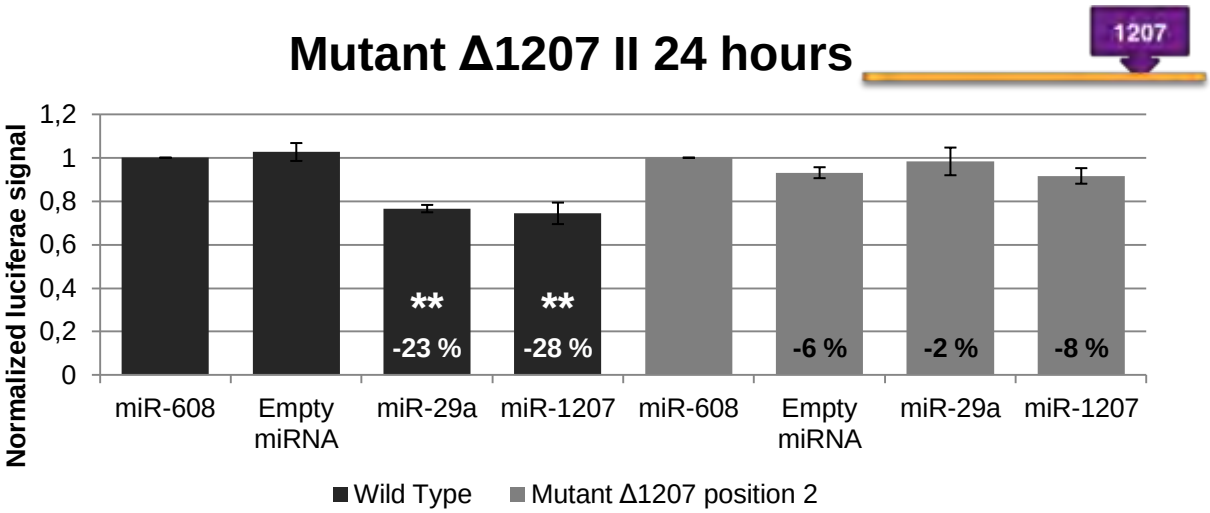


**Figure 41 Comparison of the Luciferase assay results between the wild type 3' UTR and the mutant for the 2nd site of miR-1207. In every comparison we see the percentage of difference between the negative control and the different conditions. P-value was calculated using unpaired t-test with one tail for samples with unequal variance. One star indicates P-value ≤ 0.05. Results are derived from three biological replicates for each (wild type and mutant).**

# 6. Conclusions and future prospective

We used overexpressing vectors containing the precursor region of miR-29a and miR-1207. Our goal was to investigate possible interactions of the 3' UTR of PARN and these specific miRNAs. Using the 3' UTR of PARN we were able to see an interaction of the region with the miRNAs of interest, miR-29a and miR-1207. This interaction was seen using fragments of the 3' UTR containing each time one site for one miRNA but also by using the total 3' UTR. The reductions observed were strong and statistically significant.

The construction of single mutants did show a relief of the reduction but this was not a specific event against a particular miRNA. In the future a Luciferase assay must be performed on the double mutants. The results of this experiment might enable us to clarify why we do not see a specific relief and shed some more light on the interactions of our miRNAs of interest and the PARN mRNA. Furthermore a repeatition of the Luciferase assays performed on the single mutants should be considered in order to validate the results shown in this thesis. Moreover it is important to obtain proof of the effects on the endogenous PARN, while over expressing the miRNAs, both in protein and mRNA levels. Another interesting experiment would be the use of LNA inhibitors, in Luciferase experiments as the ones described above, that can be used on cell lines, supposing they have a good basal level of expression of one of the miRNAs of interest every time, to sequestrate the miRNA and thus induce the opposite effect from what we observed in this thesis, meaning an increase of the Luciferase signal and not a reduction. This requires of course the discovery of cell line that shows good levels of endogenous miR-1207.

# 7. Bibliography


1. Lee, R. C., Feinbaum, R. L. & Ambros, V. The C. elegans heterochronic gene lin-4 encodes small RNAs with antisense complementarity to lin-14. *Cell* **75,** 843–54 (1993).

2. Almeida, M. I., Reis, R. M. & Calin, G. a. MicroRNA history: discovery, recent applications, and next frontiers. *Mutat. Res.* **717,** 1–8 (2011).

3. Reinhart, B. J. *et al.* The 21-nucleotide let-7 RNA regulates developmental timing in Caenorhabditis elegans. *Nature* **403,** 901–6 (2000).

4. Filipowicz, W., Bhattacharyya, S. N. & Sonenberg, N. Mechanisms of post-transcriptional regulation by microRNAs: are the answers in sight? *Nat. Rev. Genet.* **9,** 102–14 (2008).

5. Bartel, D. P., Lee, R. & Feinbaum, R. MicroRNAs : Genomics , Biogenesis , Mechanism , and Function Genomics : The miRNA Genes. **116,** 281–297 (2004).

6. Kozomara, A. & Griffiths-Jones, S. miRBase: annotating high confidence microRNAs using deep sequencing data. *Nucleic Acids Res.* **42,** D68–73 (2014).

7. Cai, X., Hagedorn, C. H. & Cullen, B. R. Human microRNAs are processed from capped, polyadenylated transcripts that can also function as mRNAs. *RNA* **10,** 1957–66 (2004).

8. Lee, Y. *et al.* MicroRNA genes are transcribed by RNA polymerase II. *EMBO J.* **23,** 4051–60 (2004).

9. Borchert, G. M., Lanier, W. & Davidson, B. L. RNA polymerase III transcribes human microRNAs. *Nat. Struct. Mol. Biol.* **13,** 1097–101 (2006).

10. Saito, Y. *et al.* Specific activation of microRNA-127 with downregulation of the proto-oncogene BCL6 by chromatin-modifying drugs in human cancer cells. *Cancer Cell* **9,** 435–43 (2006).

11. Brueckner, B. *et al.* The human let-7a-3 locus contains an epigenetically regulated microRNA gene with oncogenic function. *Cancer Res.* **67,** 1419–23 (2007).

12. Lujambio, A. *et al.* A microRNA DNA methylation signature for human cancer metastasis. *Proc. Natl. Acad. Sci. U. S. A.* **105,** 13556–61 (2008).

13. Denli, A. M., Tops, B. B. J., Plasterk, R. H. a, Ketting, R. F. & Hannon, G. J. Processing of primary microRNAs by the Microprocessor complex. *Nature* **432,** 231–5 (2004).

14. Yi, R., Qin, Y., Macara, I. G. & Cullen, B. R. Exportin-5 mediates the nuclear export of pre-microRNAs and short hairpin RNAs. *Genes Dev.* **17,** 3011–6 (2003).

15. Lund, E., Güttinger, S., Calado, A., Dahlberg, J. E. & Kutay, U. Nuclear export of microRNA precursors. *Science* **303,** 95–8 (2004).

16. Bohnsack, M. T., Czaplinski, K. & Gorlich, D. Exportin 5 is a RanGTP-dependent dsRNA-binding protein that mediates nuclear export of pre-miRNAs. *RNA* **10,** 185–91 (2004).

17. Hwang, H.-W., Wentzel, E. A. & Mendell, J. T. A hexanucleotide element directs microRNA nuclear import. *Science* **315,** 97–100 (2007).

18. Chendrimada, T. P. *et al.* TRBP recruits the Dicer complex to Ago2 for microRNA processing and gene silencing. *Nature* **436,** 740–4 (2005).

19. Haase, A. D. *et al.* TRBP, a regulator of cellular PKR and HIV-1 virus expression, interacts with Dicer and functions in RNA silencing. *EMBO Rep.* **6,** 961–7 (2005).

20. Lee, Y. *et al.* The role of PACT in the RNA silencing pathway. *EMBO J.* **25,** 522–32 (2006).

21. Siomi, H. & Siomi, M. C. Posttranscriptional Regulation of MicroRNA Biogenesis in Animals. *Mol. Cell* **38,** 323–332 (2010).

22. Schwarz, D. S. *et al.* Asymmetry in the assembly of the RNAi enzyme complex. *Cell* **115,** 199–208 (2003).

23. Khvorova, A., Reynolds, A. & Jayasena, S. D. Functional siRNAs and miRNAs exhibit strand bias. *Cell* **115,** 209–16 (2003).

24. Lopez-Serra, P. & Esteller, M. DNA methylation-associated silencing of tumor-suppressor microRNAs in cancer. *Oncogene* **31,** 1609–1622 (2012).

25. Weber, B., Stresemann, C., Brueckner, B. & Lyko, F. Methylation of Human MicroRNA Genes in Normal and Neoplastic Cells. *Cell Cycle* **6,** 1001–1005 (2007).

26. Jansson, M. D. & Lund, A. H. MicroRNA and cancer. *Mol. Oncol.* **6,** 590–610 (2012).

27. Kumar, M. S., Lu, J., Mercer, K. L., Golub, T. R. & Jacks, T. Impaired microRNA processing enhances cellular transformation and tumorigenesis. *Nat. Genet.* **39,** 673–677 (2007).

28. Kumar, M. S. *et al.* Dicer1 functions as a haploinsufficient tumor suppressor. *Genes Dev.* **23,** 2700–2704 (2009).

29. Esau, C. *et al.* MicroRNA-143 regulates adipocyte differentiation. *J. Biol. Chem.* **279,** 52361–5 (2004).

30. Krützfeldt, J. *et al.* Specificity, duplex degradation and subcellular localization of antagomirs. *Nucleic Acids Res.* **35,** 2885–92 (2007).

31. Elmén, J. *et al.* Antagonism of microRNA-122 in mice by systemically administered LNA-antimiR leads to up-regulation of a large set of predicted target mRNAs in the liver. *Nucleic Acids Res.* **36,** 1153–62 (2008).

32. Esau, C. *et al.* miR-122 regulation of lipid metabolism revealed by in vivo antisense targeting. *Cell Metab.* **3,** 87–98 (2006).

33. Farazi, T. A., Hoell, J. I., Morozov, P. & Tuschl, T. MicroRNA Cancer Regulation. **774,** 1–20 (2013).

34. Wittmann, J. & Jäck, H.-M. Serum microRNAs as powerful cancer biomarkers. *Biochim. Biophys. Acta* **1806,** 200–7 (2010).

35. Cortez, M. A. & Calin, G. A. MicroRNA identification in plasma and serum: a new tool to diagnose and monitor diseases. *Expert Opin. Biol. Ther.* **9,** 703–711 (2009).

36. Chim, S. S. C. *et al.* Detection and characterization of placental microRNAs in maternal plasma. *Clin. Chem.* **54,** 482–90 (2008).

37. Lawrie, C. H. *et al.* Detection of elevated levels of tumour-associated microRNAs in serum of patients with diffuse large B-cell lymphoma. *Br. J. Haematol.* **141,** 672–5 (2008).

38. Aström, J., Aström, A. & Virtanen, A. In vitro deadenylation of mammalian mRNA by a HeLa cell 3' exonuclease. *EMBO J.* **10,** 3067–71 (1991).

39. Moser, M. J., Holley, W. R., Chatterjee, A. & Mian, I. S. The proofreading domain of Escherichia coli DNA polymerase I and other DNA and/or RNA exonuclease domains. *Nucleic Acids Res.* **25,** 5110–8 (1997).

40. Zuo, Y. & Deutscher, M. P. Exoribonuclease superfamilies: structural analysis and phylogenetic distribution. *Nucleic Acids Res.* **29,** 1017–26 (2001).

41. Balatsos, N. A. A., Maragozidis, P., Anastasakis, D. & Stathopoulos, C. Modulation of poly(A)-specific ribonuclease (PARN): current knowledge and perspectives. *Curr. Med. Chem.* **19,** 4838–49 (2012).

42. Wu, M. *et al.* Structural insight into poly(A) binding and catalytic mechanism of human PARN. *EMBO J.* **24,** 4082–93 (2005).

43. Wu, M. *et al.* Structural basis of m(7)GpppG binding to poly(A)-specific ribonuclease. *Structure* **17,** 276–86 (2009).

44. Niedzwiecka, A., Lekka, M., Nilsson, P. & Virtanen, A. Global architecture of human poly(A)-specific ribonuclease by atomic force microscopy in liquid and dynamic light scattering. *Biophys. Chem.* **158,** 141–9 (2011).

45. Lejeune, F., Li, X. & Maquat, L. E. Nonsense-mediated mRNA decay in mammalian cells involves decapping, deadenylating, and exonucleolytic activities. *Mol. Cell* **12,** 675–87 (2003).

46. Korner, C. G. *et al.* The deadenylating nuclease (DAN) is involved in poly(A) tail removal during the meiotic maturation of Xenopus oocytes. *EMBO J.* **17,** 5427–5437 (1998).

47. Copeland, P. R. & Wormington, M. The mechanism and regulation of deadenylation: identification and characterization of Xenopus PARN. *RNA* **7,** 875–886 (2001).

48. Lingenfelter, B. M. *et al.* Changes of maternal transcripts in oocytes from persistent follicles in cattle. *Mol. Reprod. Dev.* **74,** 265–272 (2007).

49. Chiba, Y. *et al.* AtPARN is an essential poly(A) ribonuclease in Arabidopsis. *Gene* **328,** 95–102 (2004).

50. Chou, C.-F. *et al.* Tethering KSRP, a decay-promoting AU-rich element-binding protein, to mRNAs elicits mRNA decay. *Mol. Cell. Biol.* **26,** 3695–3706 (2006).

51. Cevher, M. A. *et al.* Nuclear deadenylation/polyadenylation factors regulate 3' processing in response to DNA damage. *EMBO J.* **29,** 1674–87 (2010).

52. Reinhardt, H. C. *et al.* DNA damage activates a spatially distinct late cytoplasmic cell-cycle checkpoint network controlled by MK2-mediated RNA stabilization. *Mol. Cell* **40,** 34–49 (2010).

53. Yoda, M. *et al.* Poly(A)-specific ribonuclease mediates 3'-end trimming of argonaute2-cleaved precursor microrna. *Cell Rep.* **5,** 715–726 (2013).

54. Kim, W.-C. & Lee, C. H. The role of mammalian ribonucleases (RNases) in cancer. *Biochim. Biophys. Acta* **1796,** 99–113 (2009).

55. Maragozidis, P. *et al.* Alterations of deadenylase expression in acute leukemias: evidence for poly(a)-specific ribonuclease as a potential biomarker. *Acta Haematol.* **128,** 39–46 (2012).

56. Clemens, M. J. & Williams, B. R. G. Inhibition of cell-free protein synthesis by pppA2′ p5′ A2′ p5′ A: a novel oligonucleotide synthesized by interferon-treated L cell extracts. *Cell* **13,** 565–572 (1978).

57. Sidrauski, C. & Walter, P. The Transmembrane Kinase Ire1p Is a Site-Specific Endonuclease That Initiates mRNA Splicing in the Unfolded Protein Response. *Cell* **90,** 1031–1039 (1997).

58. Peng, Y. & Schoenberg, D. R. c-Src activates endonuclease-mediated mRNA decay. *Mol. Cell* **25,** 779–87 (2007).

59. Song, J.-J., Smith, S. K., Hannon, G. J. & Joshua-Tor, L. Crystal structure of Argonaute and its implications for RISC slicer activity. *Science* **305,** 1434–7 (2004).

60. Liu, J. *et al.* Argonaute2 is the catalytic engine of mammalian RNAi. *Science* **305,** 1437–41 (2004).

61. Fabian, M. R. *et al.* miRNA-mediated deadenylation is orchestrated by GW182 through two conserved motifs that interact with CCR4-NOT. *Nat. Struct. Mol. Biol.* **18,** 1211–7 (2011).

62. Paschoud, S. *et al.* Destabilization of interleukin-6 mRNA requires a putative RNA stem-loop structure, an AU-rich element, and the RNA-binding protein AUF1. *Mol. Cell. Biol.* **26,** 8228–41 (2006).

63. Gherzi, R. *et al.* The RNA-binding protein KSRP promotes decay of beta-catenin mRNA and is inactivated by PI3K-AKT signaling. *PLoS Biol.* **5,** e5 (2006).

64. Pulcrano, G. *et al.* PLAUF binding to the 3'UTR of the H3.3 histone transcript affects mRNA stability. *Gene* **406,** 124–33 (2007).

65. Parker, R. & Song, H. The enzymes and control of eukaryotic mRNA turnover. *Nat. Struct. Mol. Biol.* **11,** 121–7 (2004).

66. Winter, J., Jung, S., Keller, S., Gregory, R. I. & Diederichs, S. Many roads to maturity: microRNA biogenesis pathways and their regulation. *Nat. Cell Biol.* **11,** 228–34 (2009).

67. DENTI, M., ROSA, A., STHANDIER, O., DEANGELIS, F. & BOZZONI, I. A new vector, based on the PolII promoter for the U1 snRNA gene, for the expression of siRNAs in mammalian cells. *Mol. Ther.* **10,** 191–199 (2004).